Diploma Thesis

Concept development for the design of a permeable paving stone

Submitted in satisfaction of the requirements for the degree of
Diplom-Ingenieur
of the TU Wien, Faculty of Civil Engineering

DIPLOMARBEIT

Konzeptprüfung für die Gestaltung eines durchlässigen Pflastersteins

ausgeführt zum Zwecke der Erlangung des akademischen Grades eines
Diplom-Ingenieurs
eingereicht an der Technischen Universität Wien, Fakultät für Bauingenieurwesen

von

Meriton Ramizi, Bsc.
Matr.Nr.: 1526695

unter der Anleitung von

Dipl.- Ing. Dr.techn. **Johannes KIRNBAUER**
Ass.Prof. Dr. **Teresa Liberto**
Univ.-Prof. PhD **Agathe Robisson**

Institut für Werkstofftechnologie, Bauphysik und Bauökologie
Forschungsbereich Baustofflehre, Werkstofftechnologie
Technische Universität Wien,
Lilienthalgasse 14,1030 Wien, Österreich

Wien, im Juni 2022

ABSTRACT

One of the most essential requirements for construction industry is the drainage of water from pavement and is often achieved through water permeable structures. This thesis reports on the production of water permeable pavers used for the construction of sidewalks, parking lots, and driveways.

The water-permeable pavers are built using aggregates which are held together by binding material (cement, silica fume, superplasticizer, and water). The formation of paving blocks was explored by using different types of aggregate, namely i) River aggregate (RA) 1-3 mm, ii) Crushed aggregate (CA) 2-4 mm, iii) CA 3-5 mm and iv) CA 4-8 mm. A block of paver with the aggregate and binding material was produced by putting them into a mold and applying compaction (with a weight) and vibration (using a vibrating table) simultaneously.

An essential part of the research was to optimize the quantity of binding material (cement slurry) in a block. The amount of binding material should be sufficient to provide required mechanical strength by binding the aggregates together, while at the same time does not occupy all the interparticle voids of the aggregates (which would limit water flowability).

To achieve this, different binder recipes were explored (with varying W/C ratios and amounts of admixtures) until the consistency of the binding material was optimized (zero spread). The physical properties of the aggregates, such as moisture content, water absorption, particle densities, solid volume fraction, bulk density, and void content, were investigated to study their impact on mechanical properties and water permeability of pavers.

Through this research, a conclusion was drawn to optimize the mixing proportion. The appropriate mixing proportion was 28-35% of cement paste related to the mass of the aggregate. To ensure adequate water permeability, the pavers should have a void content of at least 20% and to ensure required mechanical strength, it should be no more than 30%. The mix design proposed in this thesis was able to achieve these goals and can be used in the near future by industry to produce commercial water permeable pavers.

KURZFASSUNG

Eine der wichtigsten Anforderungen im Baugewerbe ist die Ableitung von Wasser aus dem Straßenbelag, was häufig durch wasserdurchlässige Strukturen erreicht wird. In dieser Arbeit wird über die Herstellung von wasserdurchlässigen Pflastersteinen berichtet, die für den Bau von Gehwegen, Parkplätzen und Einfahrten verwendet werden.

Die wasserdurchlässigen Pflastersteine werden aus Gesteinskörnungen hergestellt, die durch Bindemittel (Zement, Silikastaub, Fließmittel und Wasser) zusammengehalten werden. Die Bildung von Pflastersteinen wurde unter Verwendung verschiedener Arten von Zuschlagstoffen untersucht, nämlich i) Rundkorn (RK) 1-3 mm, ii) gebrochener Kantkorn (KK) 2-4 mm, iii) KK 3-5 mm und iv) KK 4-8 mm. Für die Herstellung eines Pflastersteins, wurde die Gesteinskörnungen als auch das Bindemittel in eine Schalung gegeben, gleichzeitig verdichtet (mit einem Gewicht) sowie gerüttelt (mit einer Rüttelplatte).

Ein wesentlicher Teil der Forschung bestand darin, die Menge des Bindemittels (Zementsleim) in einem Block zu optimieren. Die Menge des Bindemittels sollte ausreichen, um die erforderliche mechanische Festigkeit zu gewährleisten, indem es die Gesteinskörnungen zusammenbindet, gleichzeitig aber nicht alle Hohlräume zwischen den Partikeln der Gesteinskörnungen ausfüllt, welche sonst die Fließfähigkeit des Wassers einschränken würde.

Um dies zu erreichen, wurden verschiedene Bindemittelrezepturen untersucht (mit unterschiedlichen W/C-Verhältnissen und Mengen an Zusatzstoffen), bis die Konsistenz des Bindemittels optimiert war (keine Ausbreitung). Die physikalischen Eigenschaften der Gesteinskörnung, wie Feuchtigkeitsgehalt, Wasseraufnahme, Partikeldichten, Feststoffvolumenanteil, Schüttdichte und Hohlraumgehalt, wurden untersucht, um ihren Einfluss auf die mechanischen Eigenschaften und die Wasserdurchlässigkeit der Pflastersteine zu studieren.

Durch diese Forschung wurde eine Schlussfolgerung zur Optimierung des Mischungsverhältnisses gezogen. Das passende Mischungsverhältnis lag bei 28-35 % Zementleim, bezogen auf die Masse der Gesteinskörnung. Um eine ausreichende Wasserdurchlässigkeit zu gewährleisten, sollten die Pflastersteine einen Hohlraumgehalt von mindestens 20 % aufweisen, und um die erforderliche mechanische Festigkeit zu gewährleisten, sollte dieser nicht mehr als 30 % betragen.

ACKNOWLEDGMENTS

First and foremost, I would like to express my sincere gratitude towards supervisor, Univ.Prof. Agathe Robisson PhD Head of Research Unit Building Materials and Technology, for giving me the opportunity to work in her team as well as guiding and motivating me throughout the preparation of this thesis.

Furthermore, I would like to thank my co-supervisors, Dipl.-Ing. Dr.techn. Johannes Kirnbauer and Assistant Prof.Dr.Teresa Liberto. for their support, suggestions, and valuable advice during this work.

I would also like to thank the laboratory engineer Benjamin Marksteiner for his help in the preparation and testing of the samples, my lab mates Univ.Ass. Dana Daneshvar, MSc, and Project. Ass. Subhransu Dhar, MSc, for the thoughtful discussions and suggestions.

Special thanks to the company “Friedl Steinwerke” for financing this project and giving me the opportunity to work with them and to learn more about the whole process of paving stone production.

Last but not least, I would like to thank my parents, brother, sister, and my friends who have always stood patiently and proudly beside me, despite the difficulties of life and the separation from them.

Table of Contents

ABSTRACT I

KURZFASSUNG II

ACKNOWLEDGMENTS II

TABLE OF CONTENTS IV

LIST OF FIGURES VI

LIST OF TABLES VIII

1. INTRODUCTION 1

2. STATE OF THE ART 3

2.1. Concrete paving stones 3

2.2. Construction methods 4

2.3. The manufacturing process of dry cast paving stones 7

3. MATERIALS AND METHODS 10

3.1. Materials 10

3.1.1. Cement 10

3.1.2. Silica Fume 11

3.1.3. Superplasticizer 12

3.2. Characterization of the aggregate 12

3.2.1. Moisture states of the aggregate and water absorption 14

3.2.2. Particle densities 16

3.2.3. Solid volume fraction, bulk density, and void content 21

3.3. Methods 25

3.3.1. Cement slurry properties 25

3.3.1.1. Mixing process 25

3.3.1.2. Cone spread test 26

3.4. Preparation and testing of the samples 27

3.4.1.1. Mixing process 27

3.4.1.2. Vibrating and compacting process 29

3.4.1.3. Flexural strength 30

3.4.1.4. Water permeability 31

4. RESULTS AND DISCUSSION 32

4.1. Slurry recipes 32

4.2. Hardened pavers properties 33

4.2.1. Impact of the cement paste quantity on the thickness of the sample 33

4.2.2. Influence of slurry quantity on flexural strength 36

4.2.3. Influence of the particle size on the flexural strength 40

5. CONCLUSIONS 42

6. REFERENCES 44

7. APPENDIX 46

7.1. Influence of slurry quantity on void distribution 46

7.2. Influence of the wall effect 48

7.3. The mixture of two types of aggregates 49

7.4. Mixture with two different aggregates 51

7.5. Particle size distribution (image analysis) 52

7.6. The derived equation for the saturated surface dry particle density 55

7.7. Excel-sheet model for mixture calculation 57

List of Figures

Fig 1. 1: Cross-section of a pervious concrete sample 2
Fig. 2. 1. Concrete paving stone laying pattern [11] 3
Fig. 2. 2 Construction recommendation for a) private areas and b) public areas [13]. 6
Fig. 2. 3. Construction recommendation for a) up to 10 vehicles max. 3.5 t a day 6
Fig. 2. 4. Concrete mix suitable for the dry casting method 7
Fig. 2. 5. The manufacturing process of paving stones [17]. 8
Fig. 2. 6. Vibrating and compacting process [7] 9
Fig. 2. 7. Water permeable pavers after vibrating and compaction 9
Fig. 3. 1. Particle size distribution for Karawanken Cement CEM I 42.5 R C3A free 11
Fig. 3. 2. Particle size distribution for Silica fume Elkem 940 U 12
Fig. 3. 3. Aggregate types 13
Fig. 3. 4: Microscopic structure of a grain 14
Fig. 3. 5. Moisture states of the aggregates 14
Fig. 3. 6. Water absorption of aggregates 15
Fig. 3. 7. Pycnometer 16
Fig. 3. 8. Microstructure of the apparent particle 17
Fig. 3. 9. Microstructure of a saturated and surface-dried particle 19
Fig. 3. 10. Microstructure of an oven-dried particle 20
Fig. 3. 11. Particle densities 20
Fig. 3. 12. Vibrating plate, steel mold, and concrete specimen for aggregate compaction 21
Fig. 3. 13. Impact of the aggregate quantity on the solids volume fraction 22
Fig. 3. 14. Void content 23
Fig. 3. 15 Bulk density of aggregates 24
Fig. 3. 16. Mortar Mixer Toni MIX Visco Expert – Model 6226 [26] 26
Fig. 3. 17 Cone spread test 26
Fig. 3. 18. EIRICH R02 Vac mixer [28] 27
Fig. 3. 19. Preparation of samples and mixing process 28
Fig. 3. 20. Vibration, compaction, and demolding processes 29
Fig. 3. 21. Image of a sample under bending load 30
Fig. 3. 22. Setup for the measurement of water permeability 31
Fig. 4. 1 Slurry mixtures 32
Fig. 4. 2. Impact of cement paste quantity on the thickness of the sample and void content 34
Fig. 4. 3. Influence of the slurry quantity on the compaction of paving stones 34

Fig. 4. 4. Impact of cement paste quantity on void content and flexural strength 35
Fig. 4. 5. Optimization of the slurry quantity (Flexural strength for CA 2-4)..... 36
Fig. 4. 6. Water permeable paving stone..... 37
Fig. 4. 7. Sample with 40 % slurry quantity related to the aggregate mass. 38
Fig. 4. 8.Sample with 35 % slurry quantity related to the aggregate mass. 39
Fig. 4. 9. Sample with 28% slurry quantity related to the aggregate mass. 39
Fig. 4. 10. Flexural strength 40
Fig. 7. 1.Sample with a content of 51.2 % slurry, based on the total mass of aggregate 46
Fig. 7.2. Sample with a content of 44.6% slurry, based on the total mass of aggregate 46
Fig. 7.3. Sample with a content of 37.9% slurry, based on the total mass of aggregate 46
Fig. 7. 4. Sample with a content of 31.3% slurry, based on the total mass of aggregate 47
Fig. 7.5. Sample with a content of 24.6% slurry, based on the total mass of aggregate 47
Fig. 7.6. Sample with the content of 17,9 % slurry, based on the total mass of aggregate 47
Fig. 7. 7. Cube and cylindrical molds 48
Fig. 7.8. Influence of the wall effect on the bulk density..... 48
Fig. 7.9. The mixture of two aggregates: Bulk density for the mixture RA 1-3 with CA 4-8 49
Fig. 7.10. The mixture of two aggregates: Void content for the mixture RA 1-3 with CA 4-8..... 49
Fig. 7.11. The mixture of two aggregates: Bulk density for the mixture RA 1-3 with RA 4-8 50
Fig. 7.12. The mixture of two aggregates: Void content for the mixture RA 1-3 with CA 4-8..... 50
Fig. 7.13. Impact of filler grain in interparticle voids 50
Fig. 7.14. Mixture with two different aggregates: Flexural strength..... 51

List of Tables

Table 2. 1. Comparison of the construction methods [13] 5
Table 2. 2. Physical properties of Karawanken Cement [18] 10
Table 3. 1.Varied parameters 25
Table 3. 2. Mixing speed 26
Table 4. 1. The mixing proportion for the slurry 32
Table 4. 2. The proportions of the mixtures for CA 3-5 mm with different quantities of cement paste 34
Table 4. 3.The mixture proportion with 40% slurry quantity 37
Table 4. 4. The mixture proportion with 35% slurry quantity 37
Table 4. 5.The mixture proportion with 28 % slurry quantity 38
Table 4. 6.Mixing properties with different aggregate sizes 41
Table 4. 7. Flexural strength and water permeability 41

1. Introduction

Nowadays, urban areas are expanding due to the growing population. The valuable green zones are being replaced by buildings and paved with impervious surfaces such as concrete and asphalt (roofs, roads, parking lots, and sidewalks), leading to high economic and environmental costs for treating the stormwater [1][2]. Typically, these surfaces absorb 70-95% of sunlight, generating an urban heat island and increasing the need for air conditioning during the summer months [3]. Moreover, the resultant high temperature adversely affects the structural performance of concrete composite used in pavements, parking lots, and sidewalks [4].

Pervious concrete has been used in England and the USA for over 30 years and studied by various researchers. However, there is not yet an optimized standard for the production of pervious concrete, as the mechanical properties, compaction processes, and mix design still need to be improved [5].

Pervious concrete can be used in various applications, including parking lots, sidewalks, patios, and low traffic roads, as a porous paving system [1]. It provides an ideal solution for communities and cities facing stormwater management issues by reducing the need for underground infrastructure, preventing water pollution, and solving drainage and stormwater runoff problems [5]. It is also called porous concrete or permeable concrete and is characterized by a high porosity with a void content typically of 15-30% by volume [1].

The voids are distributed and interconnected over the entire structure, allowing water to flow through. Fig 1. 1 shows the cross-section of a pervious concrete sample in which the aggregate covered by the cement layer (matrix) and the distribution of the voids can be seen.

The mechanical properties are directly related to the void content and the distribution of the voids. With increasing void content, the mechanical properties are decreased. The compressive strength of typical pervious concrete has been measured to be 10-35 MPa, and flexural strength is between 1-3.5 MPa. Both depend on mix composition, mix ratio, and compaction method [1][6].

A suitable mix design for permeable concrete can contain single coarse aggregates with a quantity of 1300 - 1800 kg/m³ and an aggregate-cement ratio of 4-6 by mass [3]. Generally, the water-to-cement ratio for pervious concrete is between 0.27 and 0.43, and water can be combined with an admixture (superplasticizer) to achieve the desired workability [1].

Fig 1. 1: Cross-section of a pervious concrete sample

Cement paste is one of the most critical parameters that influence the strength and permeability of the pervious concrete, and the strength of pervious concrete can be increased by tuning the following parameters [1][6].

- admixtures such as silica fume and superplasticizer
- fine aggregate to increase the contact areas between the paste and the aggregate
- polymer fibers.

This study aims at optimizing a mixture for the permeable paver stones by adding a cement paste that is fluid enough to cover the surface of the aggregates and binds them together, while not flowing during the manufacturing process (a flowing cement paste may block the open pore between the bonded aggregates). The challenge is to maintain the connectivity between the voids while retaining sufficient mechanical properties and water permeability. Experimental work was conducted to support and test the materials of this study.

This work is a cooperation between the Institute of Building Materials and Technology of the Vienna University of Technology and the corporation Friedl Steinwerke [7]. The work carried out in the corporation to optimize the mix design, the materials used, the mix proportions, and the results are not presented in this report due to confidentiality.

2. State of the art

2.1. Concrete paving stones

From using collected flagstones and cobblestones to make pavement to later hand-cutting blocks of stones to create new arrangements and form a better road surface, the history of engineering has led to the development of concrete paver blocks. Segmental pavers made of stones and clay have been around since ancient Roman times, but concrete bricks replaced them, whose manufacturing began in the Netherlands during the first half of the 20th-century[8]. Their resistance and high supply during the second world war have popularized them [9].

Nowadays, concrete stone paving gets widely used for driveways, walkways, patios, etc. Different patterns and various ways of interlocking the blocks can be applied depending on the purpose of use. Their ability to support heavy loads and get easily replaced makes paver stones the preferred solution for a durable and low-maintenance substitute of asphalt and concrete surfacing. Further benefits include slip- and skid resistance and the fact that paver blocks do not change their qualities under extreme weather conditions. Concrete stones are manufactured in various textures, colors, designs, and sizes [10].

Fig. 2. 1. Concrete paving stone laying pattern [11]

More recently, concerns about the inefficient distribution of rainwater from paver stones have been raised. Recorded flooding and environmental issues of runoff imply a reconsideration of the impermeability of the most widely known and used paver stones today [12].

2.2. Construction methods

Three different construction methods can be used depending on the design of the surfacing according to the [RVS-08.18.01]. The size of the stones, the natural ground underneath, and the choice of material should be considered as a function of the area, slope and assembly when choosing the proper construction method. It is important to be aware when heavy loads are involved, as vertical forces (from heavy vehicles) can be diverted into horizontal forces, which can cause potholes. The more load is expected on the paving, the more bedding should be considered in the road construction. Avoiding depressions on the road surface is crucial for constructing sustainable paving areas. Below are listed different building methods [13].

Unbound (Standard)

Following this method, paving stones are laid on the bedding without the addition of binders, and the joints are filled without the addition of binders. This makes the road base permeable to water [13].

Bonded structure

In this method, mortar is added to bond the paving stones to the bedding. Joint mortar is used for the joint filling, the bedding layer, base, and sub-base layer are still permeable to water (i.e., from different grain sizes)[14]. The joints can crack in case of frequent temperature fluctuations [13].

Mixed structure

No binding material is used when creating a mixed construction, but the joints are filled with the addition of binders, and the bedding layer, base, and sub-base layer are still permeable to water [14]. This method is recommended for private areas, and paving slabs thickness should be at least 14 centimeters. Joint cracks can occur according to differences in weather conditions, and certain measures should be taken when stretching is observed [13].

Table 2. 2 shows the advantages and disadvantages of each construction method.

The bonded and mixed construction methods can develop cracks, have no elasticity, and their joints are more difficult to modify or to replace than the unbound construction method. One of the most important factors is the cost, and the unbound construction method surpasses the rest in that category. On the other hand, unsealing of the surface and the more complicated

cleaning process can only be difficulties of the unbound construction method. The bonded and the mixed methods have the advantages of low growth rates on the pavement joints, and the joints also don't wash out.

Table 2. 1. Comparison of the construction methods [13]

	Unbound construction method	Bonded construction method	Mixed construction method
Standard construction method	Yes	No	No
Resilience	High	High	Low
Dimentioning & Planning	Standard	Project-related	Project-related
Elasticity	High	None	None
Visable Stress Cracks	None	Possible	Possible
Unsealing of the surface	Yes	No	No
Improvement of microclimate	Yes	No	No
Cleaning	Difficult	Simple	Simple
Growth on pavement joints	Possible	Low	Low
Washing out of the joints	Possible	No	No
Joint restructuring	Simple	Difficult	Difficult
Production costs	Low	High	High
Maintenance costs	Low	High	High
Reinstatement costs	Low	High	High

Measuring the strength of the base layer of the paving structure always starts with looking at all the materials stacked above it. According to [RVS-08.18.01] [13], there are different recommendations for the unbound construction method plan depending on the purpose of use and the load.

Private areas and public areas

When it comes to private and public areas, the three lower layers require the same steps: an unbound subbase or a frost-proof in-situ soil, followed by a 10 centimeters deep base layer, after which a non-bonded bedding layer of 3-6 centimeters is added. The top layer for private areas consists of paving stones or paving slabs. They should be thicker than 4 centimeters for private areas and thicker than 6 centimeters for public ones [13].

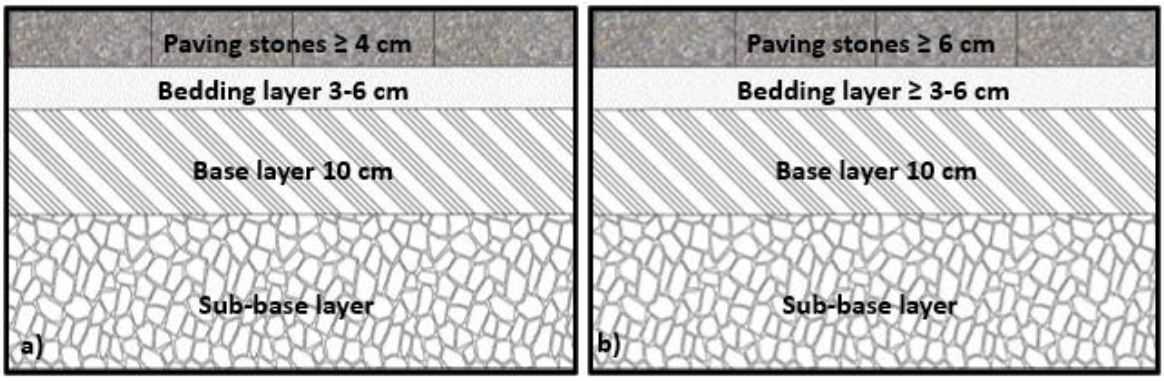

Fig. 2. 2 Construction recommendation for a) private areas and b) public areas [13].

Construction recommendations for areas driven on by vehicle

This layered structure remains similar to building roads, which get run over by many heavy vehicles, but the thicknesses change. For up to 10 cars of max. 3.5 t a day, the sub-base and bedding layer stay as described in the previous examples, while the unbound road base increases to 15 centimeters and the paving stones should be thicker than 6 centimeters. For over 10 automobiles a day, the unbound road base should be increased to 20 centimeters, and the paving stones should be thicker than 8 centimeters [13].

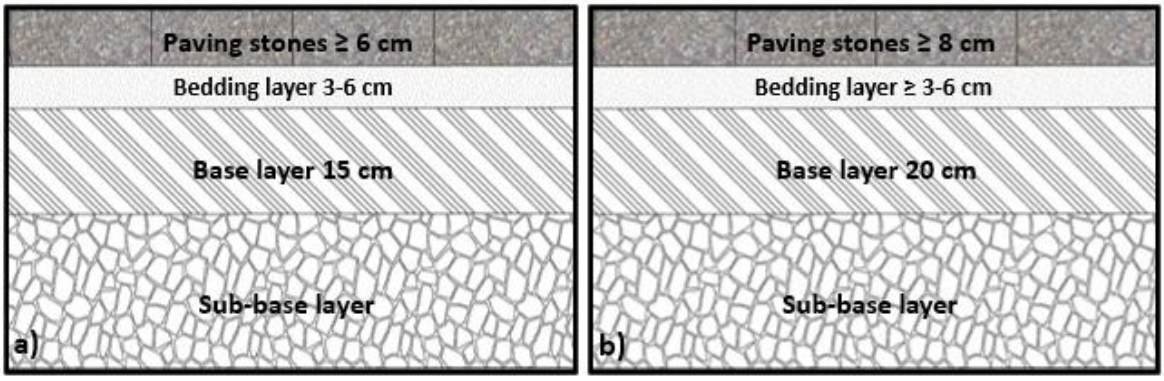

Fig. 2. 3. Construction recommendation for a) up to 10 vehicles max. 3.5 t a day and b) over 10 vehicles a day max. 3.5 t a day [13].

[RVS-03.08.63] provides more detailed information on the required thicknesses of the single layers depending on the traffic load, load class, and vehicle category [15].

Requirements and test methods for concrete paving stones are specified in [OENORM_EN_1338] [16].

2.3. The manufacturing process of dry cast paving stones

Dry-cast pavers typically have a stiff consistency that is characterized by zero slump. The mix design is very dry with low water to cement ratio. Paving stone mix design is often referred to as earth-moist, and the moisture content of the mixture usually varies in the range of 7-12%. The advantage of the dry casting method is that the mold can be removed immediately after the compaction and vibration process.

Fig. 2. 4. Concrete mix suitable for the dry casting method

The paver production process can vary depending on the factory line but generally consists of six phases and is shown in Fig. 2. 5.

- Receiving and storing raw materials
- Proportioning and mixing
- Compacting, vibration, and demolding process
- Quality control
- Setting and curing process
- Automatic cubing (i.e., preparing the paver stones for shipping)

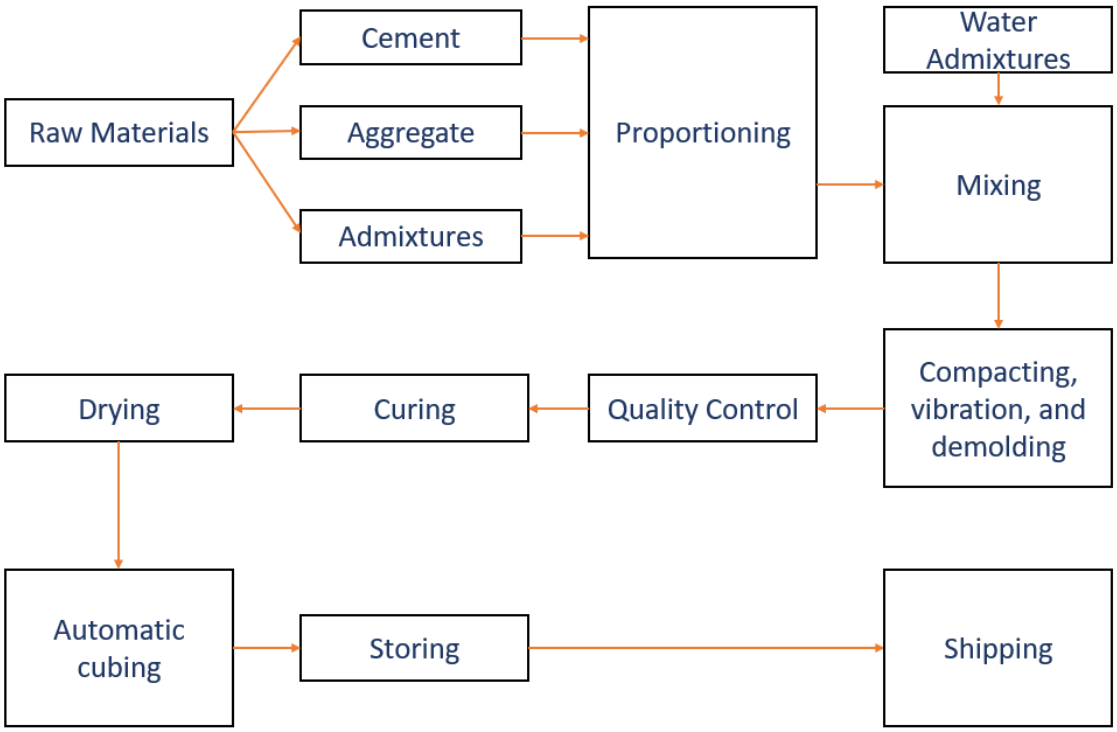

Fig. 2. 5. The manufacturing process of paving stones [17].

The proportion of materials (i.e., aggregates, cement, water, and admixtures) is predetermined and is controlled by the operator. All ingredients are mixed together, resulting in an earth-moist granular medium that can then be transferred to a mold for vibration and compaction. The mold consists of a sliding unit that holds the required amount of the mixture for filling the molds. The mixture is compacted with a hydraulic hot-stamping press and vibrated with a vibrating plate which is placed under the mold (see Fig. 2. 6). Subsequently, the mold is removed, and the pavers are transferred into the drying chamber (see Fig. 2. 7).

The vibration and compaction process is crucial for the production of concrete pavers. It has a major impact on the mechanical properties of the pavers. By increasing the compaction and vibration energy, the strength of the pavers is increased, as shown by P. Chindaprasirt et al. [5]. In the case of this study, higher compaction and vibration energy reduced the void content (i.e., cement paste flowed during the compaction and vibration process, blocking the voids), resulting in low water permeability. The main focus of this work was to develop a mixed design that is suitable for the production of permeable paving stones. In the following chapters, the materials used, methods, and results are discussed.

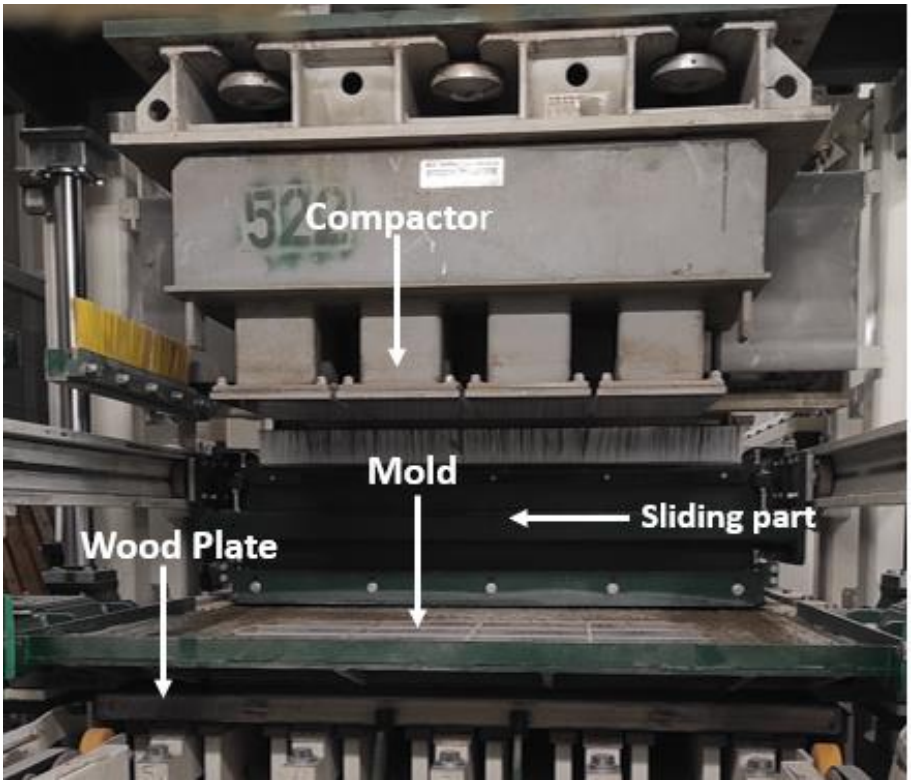

Fig. 2. 6. Vibrating and compacting process [7]

Fig. 2. 7. Water permeable pavers after vibrating and compaction process and drying chamber [7]

3. Materials and Methods

In this chapter, the materials used for making pavers (aggregates, sand, cement, additives) are described. The tools to characterize the materials and the pavement stones are also described. Unless specified, all characterization was performed in the laboratory of the Institute for Materials Technology, Building Physics, and Building Ecology of the Vienna University of Technology.

3.1. Materials

3.1.1. Cement

Karawanken cement CEM I 42.5 R, C3A free, was used. It has an increased resistance to sulfate attack and can be applied in all exposure classes [18]. The following table shows some of the physical properties of CEM I 42.5 R C3A free according to standard test EN 196.

Table 2. 2. Physical properties of Karawanken Cement [18]

Technical guide values	CEM I 42.5 R C3A free
Comp. strength after 1d	13 MPa
Comp. strength after 28d	56 MPa
Start of solidification	210 min
Particle Density	3,17 g/cm³

The distribution of particle size was measured with the Mastersizer 3000. The technique involves laser diffraction through a liquid in which the particles are suspended, measuring their size in the suspension volume. The results (i.e., particle size distribution curve) for Karawanken cement are shown in Fig. 3. 1. as an average of 5 measurements, with a D10 value of 3.69 µm, a D50 value of 13.87 µm, and a D90 value of 32.19 µm. D10, D50 and D90 means that 10, 50 and 90% of the particles have sizes below (or equal to) the respective values [22].

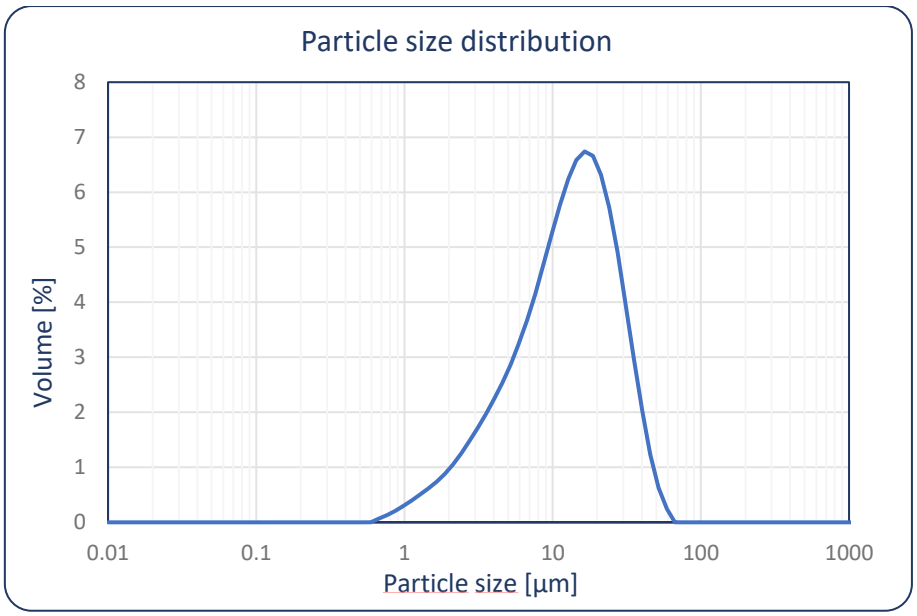

Fig. 3. 1. Particle size distribution for Karawanken Cement CEM I 42.5 R C3A free

3.1.2. Silica Fume

Silica fume (i.e., micro-silica) is an ultrafine powder with average spherical and very fine particles of 0.1 - 0.3 µm. It is a by-product of the production of silicon and ferrosilicon alloys produced in electric furnaces [19]. Typically, silica fume is used to increase strength, reduce water permeability of the matrix, increase resistance to chemical attack, and improve the durability of concrete [20]. For the experiments, silica fume powder Elkem 940 U was used. Silica fume powder has a particle density of 2.05 g/cm³ [21], and the recommended dosage is between 5-15 mass % of the binder content. The particle size distribution measured with the Mastersizer 3000 for silica fume is shown in Fig. 3. 2. as an average of 5 measurements, with a D10 value of 0.05 µm, a D50 value of 0.17 µm, and a D90 value of 0.50 µm.

D10, D50 and D90 means that 10, 50 and 90% of the particles have sizes below (or equal to) the respective values [22].

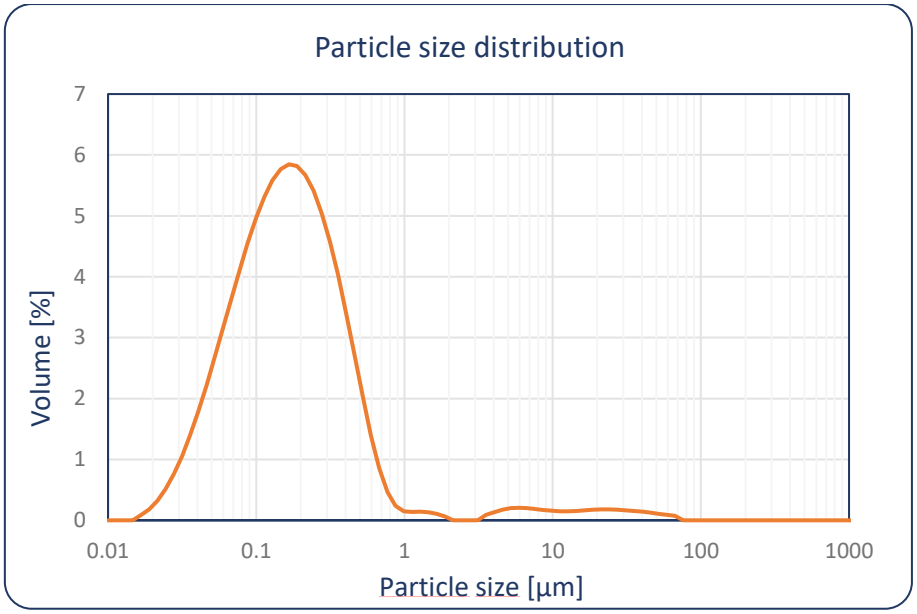

Fig. 3. 2. Particle size distribution for Silica fume Elkem 940 U

3.1.3. Superplasticizer

Superplasticizers are synthetic polymers with different lengths and structures of chains [22]. By using superplasticizers, water addition in concretes can be reduced (~30%) while maintaining low yield stress without increasing the W/C ratio [22]. A PCE-based superplasticizer (polycarboxylate ether) Master Glenium ACE 430 from BASF with a density of 1.06 g/cm³ was used for the tests. The aim of using superplasticizer was to increase the amount of cement and obtain better mechanical properties without changing the workability of the slurry. The superplasticizer was always dissolved in tap water before adding to the cement.

3.2. Characterization of the aggregate

The mechanical properties and water permeability of the pavers depend upon the size and shape of the aggregates. To study the impact of aggregate size and shape on the mechanical properties of the pavers and water permeability, different types of aggregates, such as river aggregate (RA) and crushed aggregate (CA) with different sizes as follow (Fig. 3. 3)

- RA 1-3 mm
- CA 2-4 mm
- CA 3-5 mm
- CA 4-8 mm

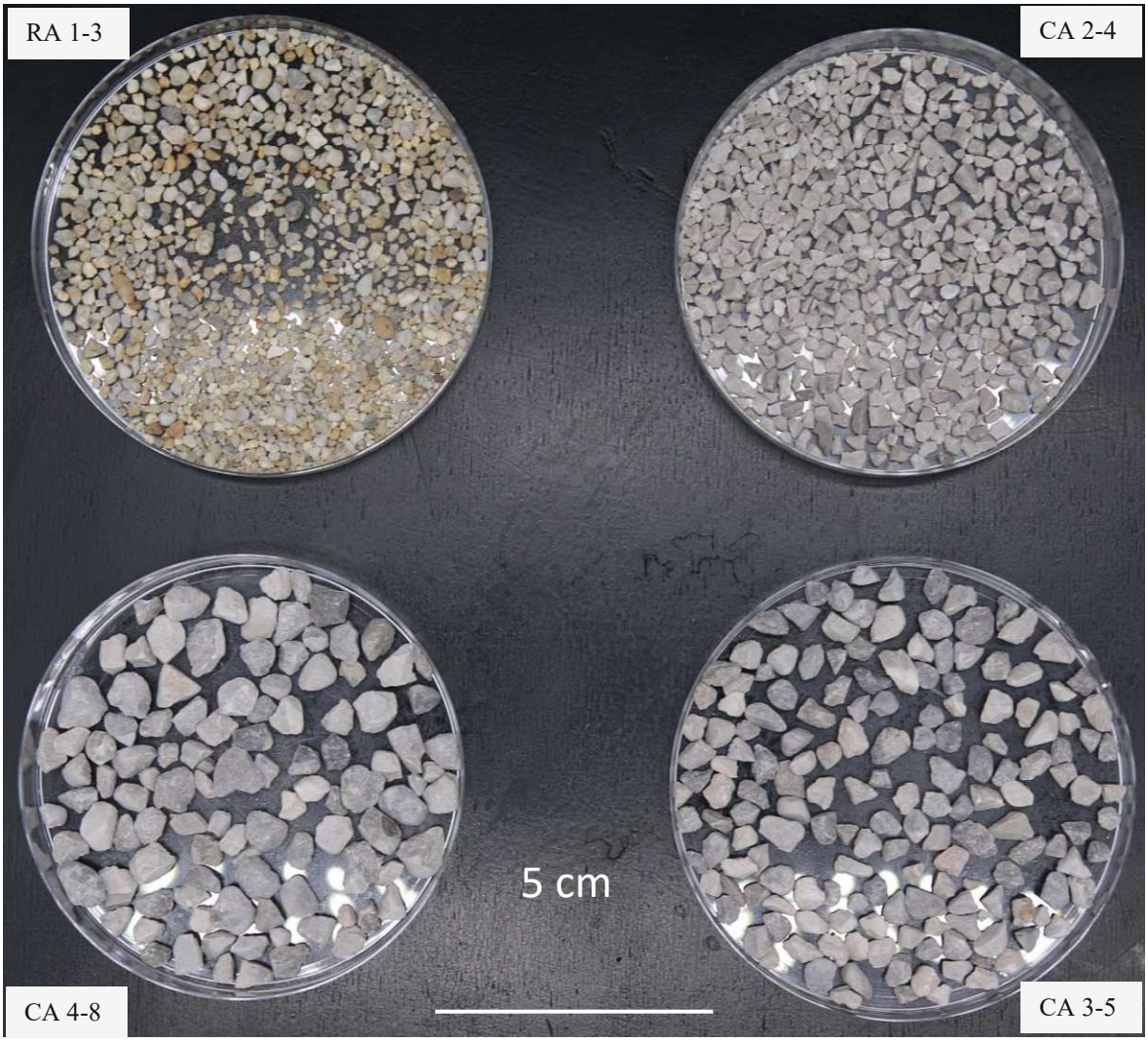

Fig. 3. 3. Aggregate types

This subsection describes various types of aggregate testing, including:

- Moisture states of the aggregates
- Water absorption capability
- Particle densities
- Solid volume fraction, bulk density, and void content

The moisture content and water absorption of the aggregate are key parameters for the mixture proportion, as they affect the amount of water that needs to be added to the mixture. The particle densities of the aggregate are another key parameter for appropriate mix design, as they affect the void content and solids volume fraction of the mixture, which directly affects the water permeability of the pavers.

All the above physical properties of aggregates are described in this section.

3.2.1. Moisture states of the aggregate and water absorption

At the microscopic level, an aggregate has accessible and inaccessible pores to the water. The accessible pores can be either partially or fully saturated with water.

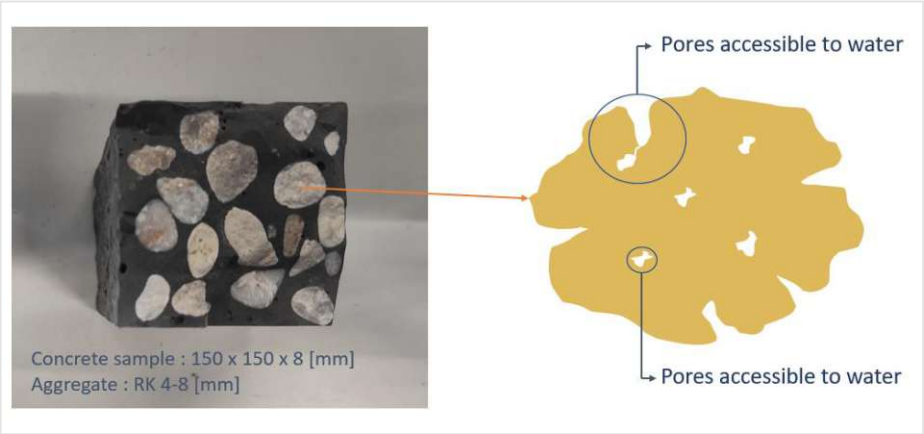

Fig. 3. 4: Microscopic structure of a grain

For this reason, ÖNORM EN 1097-6 [23] considers all moisture states, as shown in Fig. 3. 5.

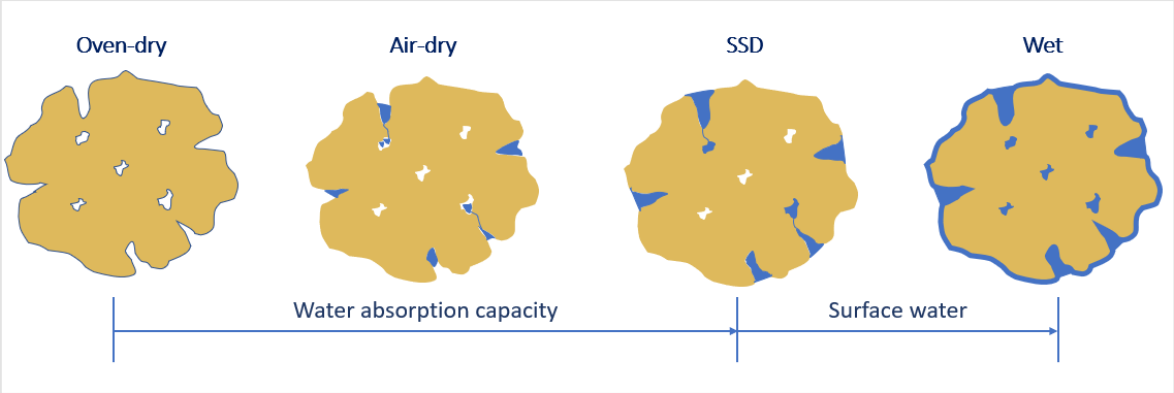

Fig. 3. 6. Moisture states of the aggregates

- **Oven dry:** The aggregate does not contain moisture (all pores are empty). The aggregate should be heated to (110 ± 5) °C until it reaches a constant mass.
- **Air dry:** The aggregate may have some moisture (some of the accessible pores are filled by the water).
- **Saturated, surface dry-(SSD):** all accessible pores are filled with water, but the main surface of the grains is dry
- **Wet:** all pores accessible to the water are filled with water, and the main surface of the grains is wet.

Water absorption capacity

For each type of aggregate, three test portions were prepared to determine the water absorption of the aggregate. The aggregates were kept in the pycnometer for 24 hours, then removed and drained for a few minutes. The test portion was placed on a dry cloth, which was used to wipe the surface of the aggregate until the SSD condition was reached. After weighing their mass, the aggregates were heated in the oven at (110 ± 5) °C until a constant mass was reached. The procedure was carried out according to ÖNORM EN 1097-6 [10] (see Annex C) to determine the water absorption of the aggregates. The water absorption after 24 hours was calculated according to equation (1), and the results obtained for the four different types of aggregates are shown in Fig. 3. 7.

$$WA_{L24} = \frac{M_1 - M_4}{M_4} \times 100 \quad (1)$$

WA_{L24} – Water absorption after 24 h, in %

M_1 – Mass of saturated and surface-dried aggregates, in grams (gr)

M_4 – Mass of dry aggregate, in grams (gr)

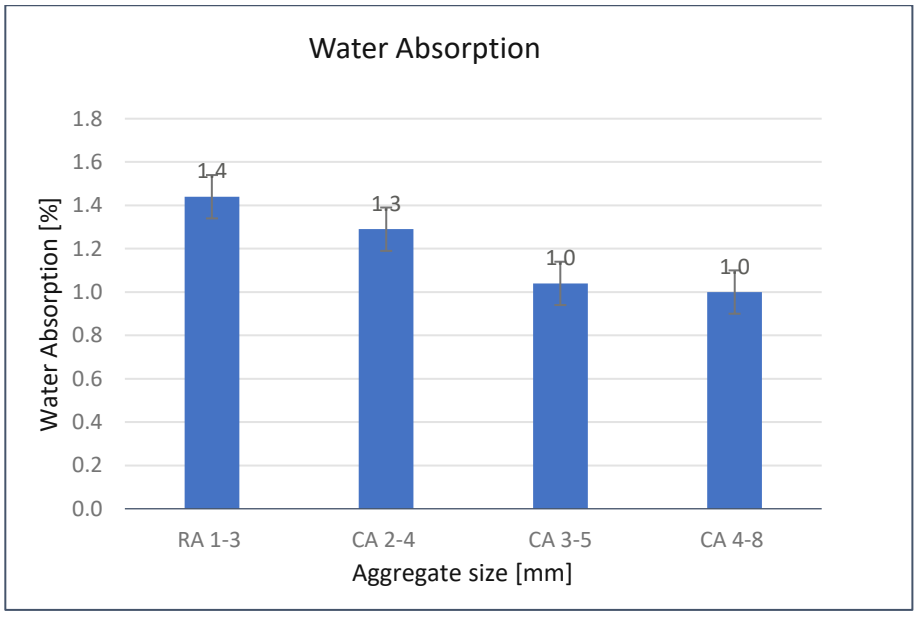

Fig. 3. 7. Water absorption of aggregates

The water absorption capacity for all aggregates is between (1.15 - 1.45) %. The river aggregate of 1-3 mm absorbs the largest amount of water after 24 hours compared to the other sizes, reaching a value of 1.44% with a deviation of ± 0.2%.

3.2.2. Particle densities

Particle density is the ratio between the mass of the aggregate and the volume of the aggregate, and its unit is [kg/m³].

$$\rho = \frac{M}{V} = \frac{Mass}{Volume} \quad (2)$$

A pycnometer in the laboratory of the TU Vienna with a volume of 1 l was used to determine the particle densities of the aggregate. Pycnometer bottles are generally made of glass and consist of the bottom flask and the funnel-shaped capillary tube that allows air bubbles to escape from the bottom flask (Fig. 3. 6). The measuring procedure was followed according to the Austrian standards ÖNORM EN 1097-6 [10] for the use of the pycnometer and the determination of particle density [10](see Annex C). The temperature of the water used for particle density measurements was always (22 ± 3) °C [10] (see Annex G).

In the below section, the following particle types of density according to the Austrian standard are explained in more detail using the pycnometer method.

Apparent particle density - ρa
Oven-dried particle density - ρrd
Saturated and surface-dried particle density - ρssd

Fig. 3. 8. Pycnometer

Apparent particle density

The apparent particle density, according to ÖNORM EN 1097-6 [10], is defined as:

"Ratio obtained by dividing the oven-dried mass of an aggregate sample by the volume it occupies in water, including the volume of any internal sealed voids but excluding the volume of water in any water accessible voids." [10] (see 3.1).

$$\rho_a = \rho_w \frac{M_4}{M_4 - (M_2 - M_3)} \quad (3)$$

ρ_a - apparent particle density, in kilograms per cubic meter (kg/m³)

ρ_w- density of water at the test temperature, in kilograms per cubic meter (kg/m³)

M_2- mass of the pycnometer containing the sample of saturated aggregate and water, in grams (gr)

M_3- mass of the pycnometer filled with water only, in grams (gr)

M_4- mass of the oven-dried test portion in air, in grams (gr)

In simplified terms, apparent particle density can be defined as the weight ratio of the oven-dried particle to the volume of the particle, including the volume of pores inaccessible to water, but excluding the volume of pores accessible to water. (see Fig. 3. 9).

$$\rho_a = \frac{M_{OD}}{V_P + V_I} \quad (4)$$

ρ_a - apparent particle density, in kilogram per cubic meter (kg/m³)

M_{OD}- mass of the oven-dried test portion in air, in kilogram (kg)

V_P- volume of the particle, in cubic meter (m³)

V_I- volume of the pores inaccessible to water, in cubic meter (m³)

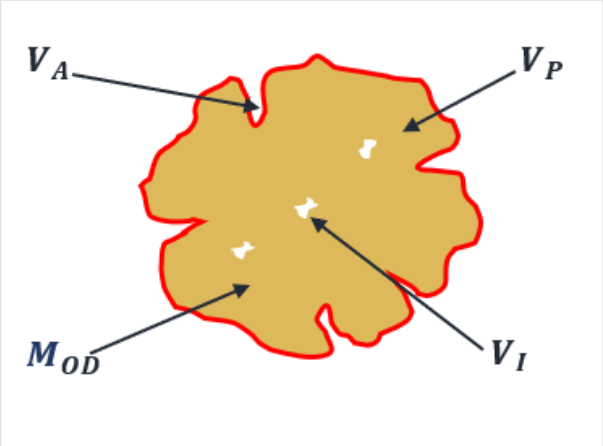

Fig. 3. 9. Microstructure of the apparent particle

The results for the apparent density of all aggregates are shown in (Fig. 3. 12).

Saturated and surface-dried particle density

The saturated and surface-dried particle density according to ÖNORM EN 1097-6 [10] is defined as:

"Ratio obtained by dividing the sum of the oven-dried mass of an aggregate sample and the mass of water in any water accessible voids by the volume it occupies in water, including the volume of any internal sealed voids and the volume of any water accessible voids" [10] *(see 3.5).*

$$\rho_{ssd} = \rho_w \frac{M_1}{M_1 - (M_2 - M_3)} \quad (5)$$

ρ_{ssd} - saturated and surface-dried particle density, in kilograms per cubic meter (kg/m³)

ρ_w- density of water at the test temperature, in kilograms per cubic meter (kg/m³)

M_1- mass of the saturated and surface-dried aggregate, in kilograms (kg)

M_2- mass of the pycnometer containing the Sample of saturated aggregate and water, in kilograms (kg)

M_3- mass of the pycnometer filled with water only, in kilograms (kg)

M_4- mass of the oven-dried test portion in air, in kilograms (kg)

In simplified terms, the saturated and surface-dried particle density can be defined as the weight ratio of the saturated and surface-dried (SSD) particle to the volume unit of the particle, including the volume of pores accessible and inaccessible to water (see Fig. 3. 10). The difference between the saturated surface-dried and the oven-dried particle density is that the mass of water in the accessible pores is considered in the SSD density.

$$\rho_{ssd} = \frac{M_{SSD}}{V_P + V_A + V_I} \quad (6)$$

ρ_{ssd} - saturated and surface-dried particle density, in kilograms per cubic meter (kg/m³)

M_{ssd}- mass of the saturated and surface-dried aggregate, in kilogram (kg)

V_P- volume of the particle, in cubic meter (m³)

V_A- volume of the pores accessible to water, in cubic meter (m³)

V_I- volume of the pores inaccessible to water, in cubic meter (m³)

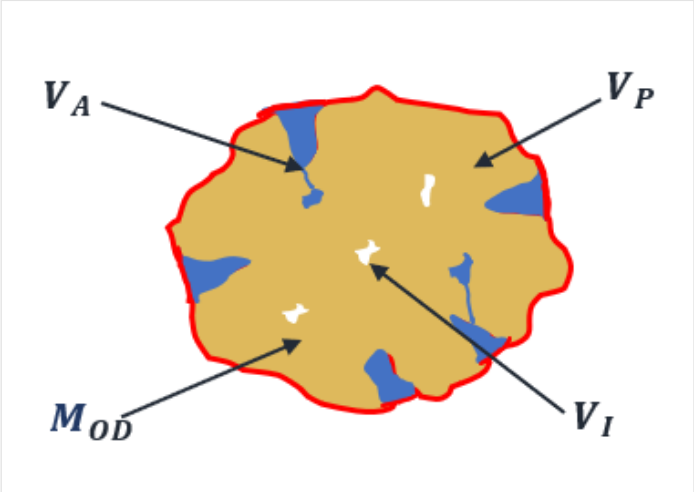

Fig. 3. 10. Microstructure of a saturated and surface-dried particle

The results for the oven-dried density of all aggregate types are shown in the (Fig. 3. 12).

Oven-dried particle density - ρa

The oven-dried particle density, according to ÖNORM EN 1097-6 [10], is defined as:

"Ratio obtained by dividing the oven-dried mass of an aggregate sample by the volume it occupies in water, including the volume of any internal sealed voids and the volume of any water accessible voids" [10] (see 3.3).

$$\rho_{rd} = \rho_w \frac{M_4}{M_1 - (M_2 - M_3)} \quad (7)$$

ρ_{rd} -the oven-dried particle density, in kilograms per cubic meter (kg/m³)

ρ_w- the density of water at the test temperature, in kilograms per cubic meter (kg/m³)

M_1-the mass of the saturated and surface-dried aggregate, in grams (gr)

M_2- the mass of the pycnometer containing the Sample of saturated aggregate and water, in grams (gr)

M_3-the mass of the pycnometer filled with water only, in grams (gr)

M_4-is the mass of the oven-dried test portion in air, in grams (gr)

In simplified terms, the oven-dried particle density can be defined as the weight ratio of the oven-dry particle to the volume unit of the particle, including the volume of pores accessible and inaccessible to water (see Fig. 3. 11).

$$\rho_{rd} = \frac{M_{OD}}{V_P + V_A + V_I} \quad (8)$$

ρ_{rd} - oven-dried particle density, in kilogram per cubic meter (kg/m³)
M_{OD}- mass of the oven-dried test portion in air, in kilogram (kg)
V_P- volume of the particle, in cubic meter(m³)
V_A- volume of the pores accessible to water, in cubic meter (m³)
V_I- volume of the pores inaccessible to water, in cubic meter (m³)

The results for the apparent oven-dried and saturated surface dry densities of all aggregates are shown in Fig. 3. 12.

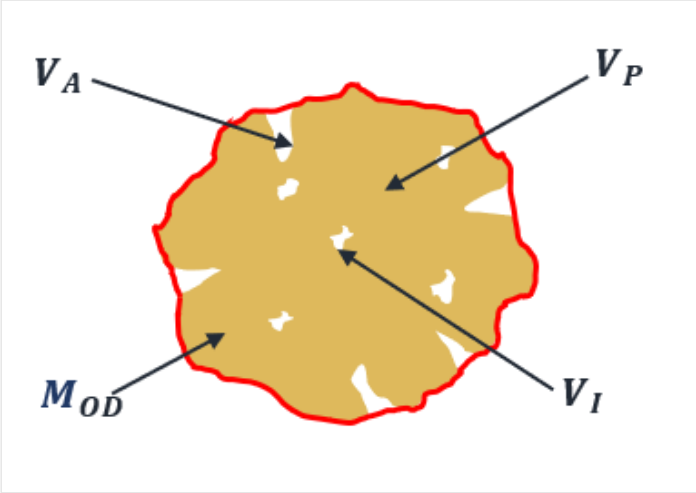

Fig. 3. 11. Microstructure of an oven-dried particle

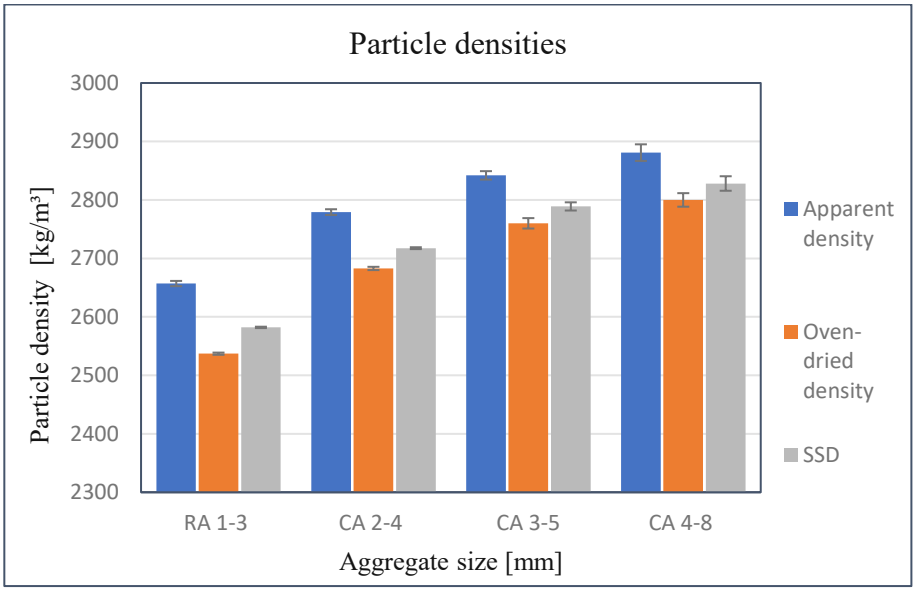

Fig. 3. 12. Particle densities

3.2.3. Solid volume fraction, bulk density, and void content

A steel mold, a vibrating plate, and a concrete cube of weight 5.6 kg (stress = 2.4 kPa) for compaction, as shown in Fig. 3. 13, were used to calculate the bulk density, solids volume fraction, and void content of a pack of aggregates.

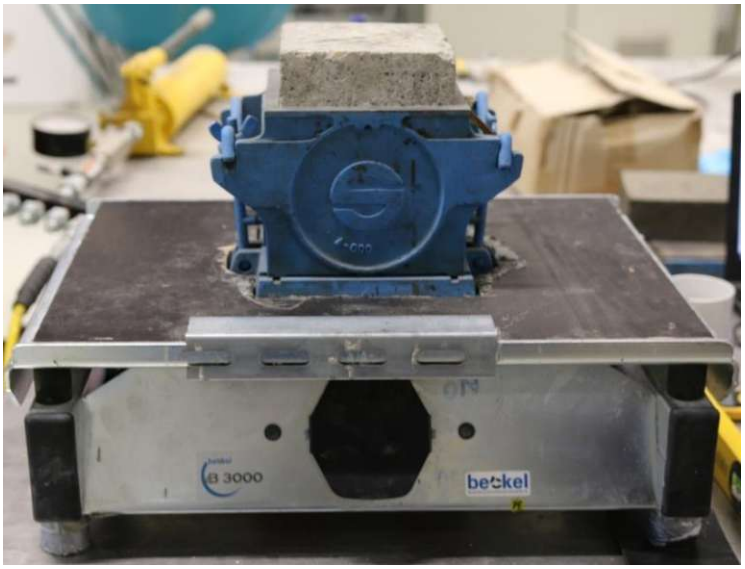

Fig. 3. 13. Vibrating plate, steel mold, and concrete specimen for aggregate compaction and vibrating

The mold was filled with a certain amount of particles (Stepwise- to determine the effect of the quantity of aggregates on the solid volume fraction). The prepared samples were vibrated and compacted for approximately 30 seconds. Then the thickness of the compacted particles was precisely measured to calculate the volume of the sample. Three samples were prepared for each measurement, and the average of all measurements was taken for the final results

Solid volume fraction

The solids volume fraction is defined as the ratio between the solids volume (sum of each individual aggregate) and the total volume (mold surface area * height of compacted sample) [24].

$$\phi = \frac{V_s}{V_{Sam}} \tag{9}$$

V_S - volume of the solid (m³)

V_{Sam} - volume of the sample (m³)

To observe the effect of the amount of aggregate on the solid volume fraction, the mold was filled (stepwise) with different amounts of aggregate (previously dried at (110 ± 5) °C), starting with 2000 g and then adding 1000 g more for each measurement until the mold was filled. The prepared samples were vibrated (vibrating plate) and compacted (concrete Sample) shown in (Fig. 3. 13) for approximately 30 seconds. The thickness of the Sample was measured precisely to calculate the volume of the Sample according to equation (10) to determine the volume fraction of the solid according to equation (9). The result is shown in (Fig. 3. 14)

$$V_S = M_{OD\,x}\,\rho_a \tag{10}$$

V_S- volume of the aggregate in cubic meter (m³)
M_{OD} - mass of the aggregate dried in oven, in kilogram (kg)
ρ_a- apparent particle density, in kilogram per cubic meter (kg/m³)

The choice of apparent density included the open pore volume in the overall volume of void. The ratio between open pores and aggregate total volume (incl. open and closed pores) being in the range of 4-6 % for all aggregate types, we can neglect the volume of aggregate open pores in the interstitial void content.

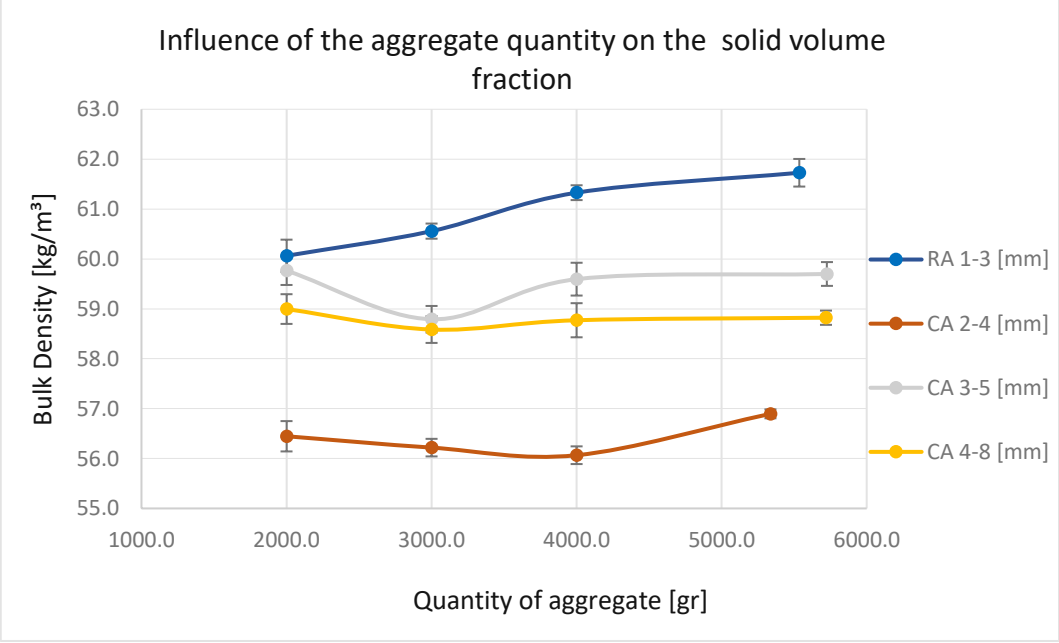

Fig. 3. 14. Impact of the aggregate quantity on the solids volume fraction

The solid volume fraction of crushed aggregates is consistently lower than the solid volume fraction of round aggregates. This result is not surprising as crushed aggregates are harder to compact due to high friction. Also, the higher the content of round aggregates, the higher the bulk density (or compaction).

Void content

The void content or porosity of the aggregate can be defined as the pore space between the particles (in our case, including the accessible pores to water), which can be filled with either air or water, and is directly related to the solid volume fraction [24] and is calculated with the following equation (11).

$$\boldsymbol{\varepsilon = 1 - \phi} \tag{11}$$

$\boldsymbol{\phi}$ −Solid volume fraction [%]

$\boldsymbol{\varepsilon}$ − Void content [%]

The average of all solid volume fraction measurements (Fig. 3. 14) was taken to calculate the void content for each aggregate type compacted following the defined procedure. The void content was calculated according to the expression (11), and the results are shown in (Fig. 3. 15). Results show that crushed aggregates compact less than the rounder river aggregates.

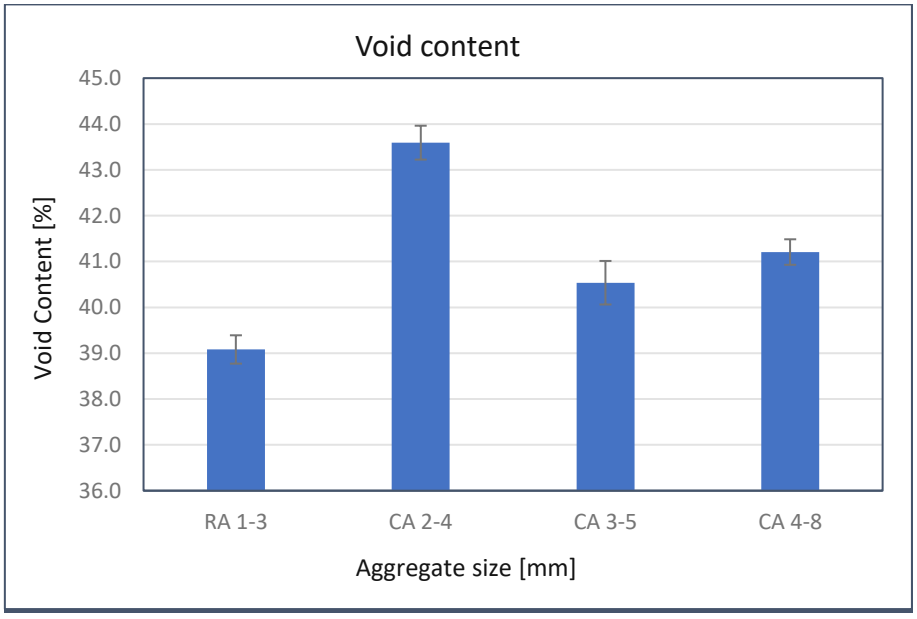

Fig. 3. 15. Void content

Bulk density

The bulk density was calculated according to the equation (12) and is defined as the ratio between the mass of the oven-dried solid and the volume of the sample [25]. sample [25]

$$\rho_b = \frac{M_{OD}}{V_A} \quad (12)$$

ρ_b - bulk density, in kilogram per cubic meter (kg/m³)
M_{OD}- mass of the oven-dried test portion, in kilogram (kg)
V_A- volume test specimen, in cubic meter(m³)

The bulk density was calculated for each slope (different aggregate type) from the measurements of the volume fraction of solids (see Fig. 3. 14), and the average of all measurements was considered for each aggregate type.

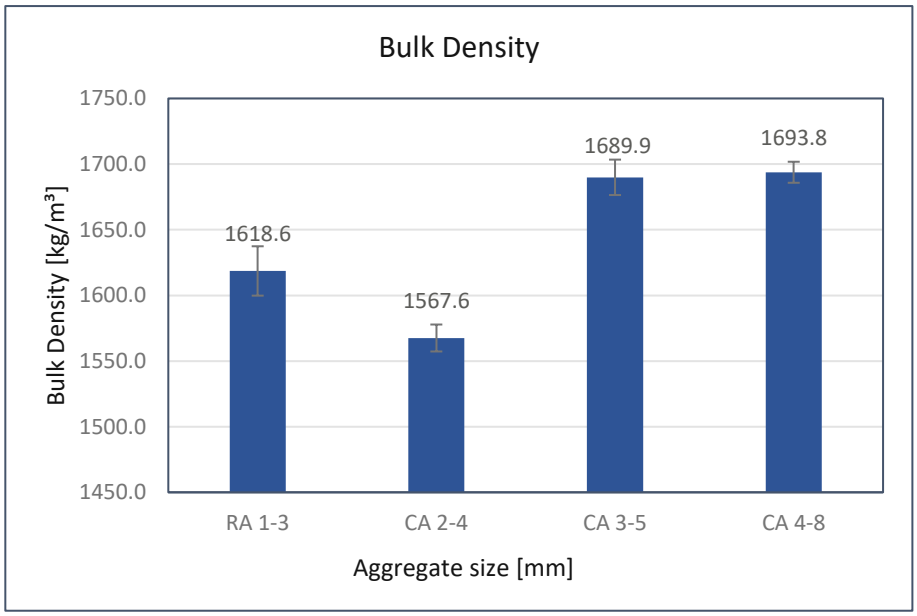

Fig. 3. 16 Bulk density of aggregates

3.3. Methods

3.3.1. Cement slurry properties

To study the fresh properties of the mortar and to investigate the influence of the mortar on the mechanical properties and water permeability of the pavers, three different mixtures were studied. The varied parameters were W/C ratio, silica fume content, and superplasticizer content. **Mix 1** consists of water and cement only, **Mix 2** consists of cement, water, and superplasticizer, and **Mix 3** consists of cement, water, silica fume, and superplasticizer.

The three mixes were designed to have zero slump to avoid the flowing of the paste during the compaction and vibration process. For **Mix 1**, a W/C ratio of 0.30 was identified. W/C ratio of 0.28 was identified by adding 0.2 % Superplasticizer based on the cement quantity for **Mix 2**. whereas, in **Mix 3,** a W/C ratio of 0.28 was identified by adding 0.7 superplasticizer and 10 % silica fume based on the quantity of cement.

Table 3. 1.Varied parameters

Varied parameters	**Mix 1**	**Mix 2**	**Mix 3**
W/C	0.30	0.28	0.28
Superplasticizer [%.M]	---	0.2	0.7
Silica fume [%.M]	---	---	10

3.3.1.1. Mixing process

For the slurry measurements, Mortar Mixer ToniMIX Visco Expert – Model 6226 [26] (Fig. 3. 17) was used. The amount of ingredients was measured and placed in the bowl, adding the amount of water carefully within 10 seconds. For **Mix 2** and **Mix 3**, superplasticizer was added to the amount of water and then to the mixing bowl.

The auto-mixing program was set according to ÖNORM EN 196-1 [27] with the following mixing order and duration:

- after the ingredients were measured and placed into the bowl, the mixing process began at low speed for 60 seconds and then at high speed for 30
- after mixing at high speed for 30 seconds, the mixer rest for 90 seconds where the slurry sticking to the wall and the bottom of the bowl was scraped and placed in the middle of the bowl with a silicone spatula

- after 90 seconds of rest, the mixing process began again for 60 seconds at high speed

Fig. 3. 17. Mortar Mixer Toni MIX Visco Expert – Model 6226 [26]

Table 3. 2.Mixing speed

Speed	Rotation $\boldsymbol{min^{-1}}$	Planetary movement $\boldsymbol{min^{-1}}$
Low	140 ± 5	62 ± 5
High	285 ± 10	125 ± 10

3.3.1.2. Cone spread test

The Hagerman cone (Fig. 3. 18) was used for this test. After the cone was filled with paste, the top was carefully leveled, and then the cone was pulled upwards. The spread diameter of the sample was measured along two diameters, and the average was calculated.

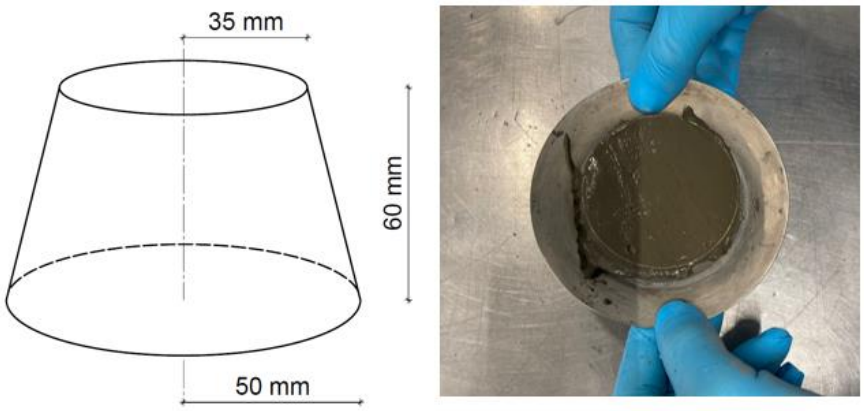

Fig. 3. 18 Cone spread test

3.4. Preparation and testing of the samples

3.4.1.1. Mixing process

The mixing process was carried out using an EIRICH R02 Vac (Fig. 3. 19) with a usable capacity of max. 5 L and a rotational capacity of 1200 rpm. Before mixing, the mixing container was always cleaned and dried. The rotation speed was set at 200 rpm, and the quantity of the mixture prepared for each experiment was V=1.5 L.

Fig. 3. 19. EIRICH R02 Vac mixer [28]

According to recipes, the required amount of cement, silica fume, and aggregates were added to the mixer (Fig. 3. 20.1) and mixed for 90 seconds, followed by the slow addition of the water/superplasticizer for ~30 sec (Fig. 3. 20.2) and all ingredients were then mixed for 90 seconds. The mixture, a granular medium made of aggregates covered with cement slurry, was quickly removed from the mixer and used for the vibration and compaction process (Fig. 3. 20.3-4).

Fig. 3. 20. Preparation of samples and mixing process

3.4.1.2. Vibrating and compacting process

To simulate the real manufacturing process of the pavers mentioned in section 2.3, a vibrating plate and a concrete sample of 5.6 kg were used to compact the mixture (Fig. 3. 21.2). The required amount of mixture was poured into the mold (Fig. 3. 21.1), compacted, and vibrated with a vibrating plate. This procedure was done in less than 120 s to avoid the drying of the slurry covering the aggregates. Immediately after, the Sample was de-molded (Fig. 3. 21.3-4) and stored in a climate chamber for three days.

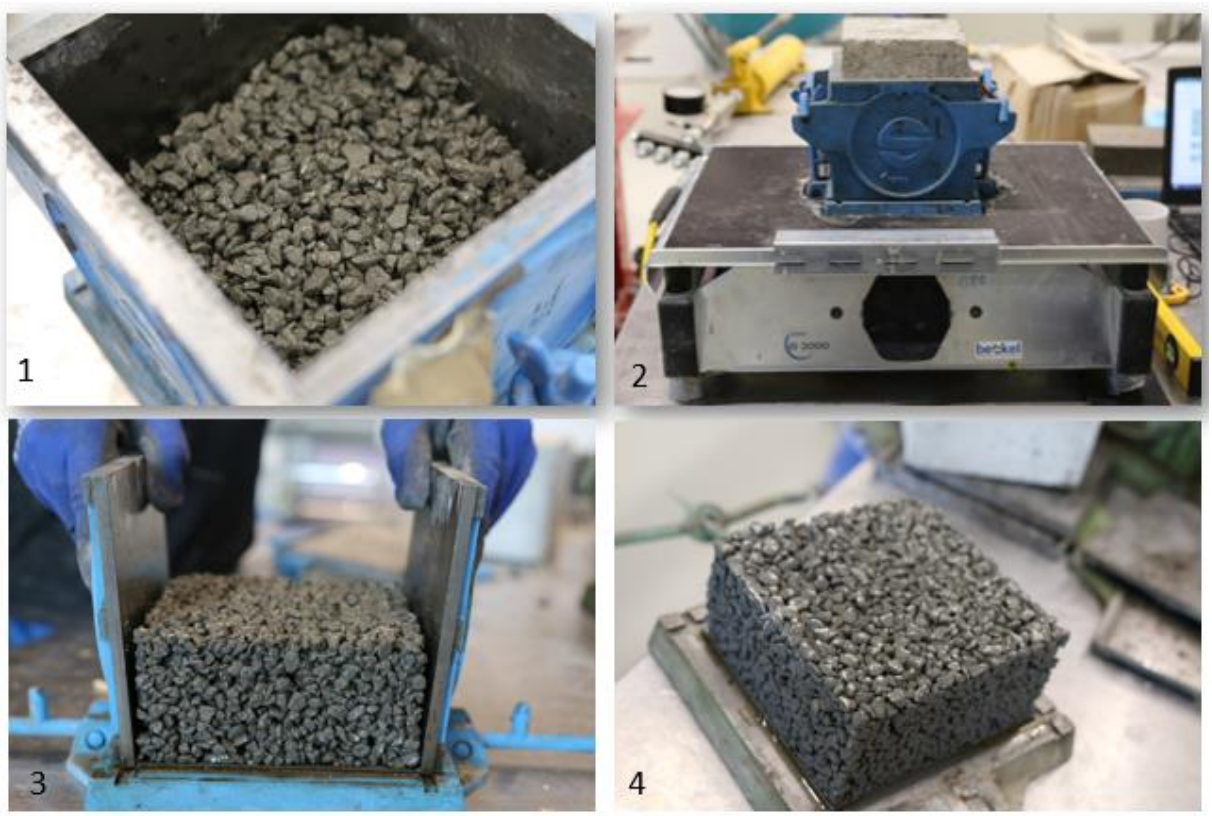

Fig. 3. 21. Vibration, compaction, and demolding processes

3.4.1.3. Flexural strength

Flexural strength, an important property for pavement stones, was determined by a three-point bending test. Before the samples were placed for testing, the thickness was accurately measured with a caliper. Specimens were tested to failure by applying a constant load of at least 50 N/s as a function of test duration. The tests were carried out using a Zwick testing. The testing of the samples is shown in Fig. 3. 22.

The flexural strength for concrete samples supported at two points, with the load applied at one point [29], can be calculated with equation (13).

$$f_{ct} = 1.5 \cdot \frac{F \cdot l}{d_1 \cdot (d_2)^2} \qquad (13)$$

f_{ct}- flexural strength [MPa]
F - maximum load applied [N]
l - distance between the support rollers [mm]
d_1-width of the cross-section [mm]
d_2-the height of the cross-section [mm]

Fig. 3. 22. Image of a sample under bending load

3.4.1.4. Water permeability

To estimate the water permeability of the produced pavement stones, a setup with impermeable wooden boards was constructed, as shown in Fig. 3. 23. The sample was placed in the test setup and sealed with silicon. The setup was inserted into a 1 m long pipe. Finally, the pipe was filled with water, and the time it took for the water to pass through the sample was measured. From the time measurement, permeability to water was calculated [l/s/m²].
A similar method is used to measure the permeability of the soil in the following work [30].

Fig. 3. 23. Setup for the measurement of water permeability

4. Results and Discussion

4.1. Slurry recipes

Aiming to reduce the flowing of the slurry during the vibration and compaction process, three different slurries were optimized. Table 4. 1 the mixing proportion of the slurry for 1 dm³ and Fig. 4. 1 shows the spread of the slurry.

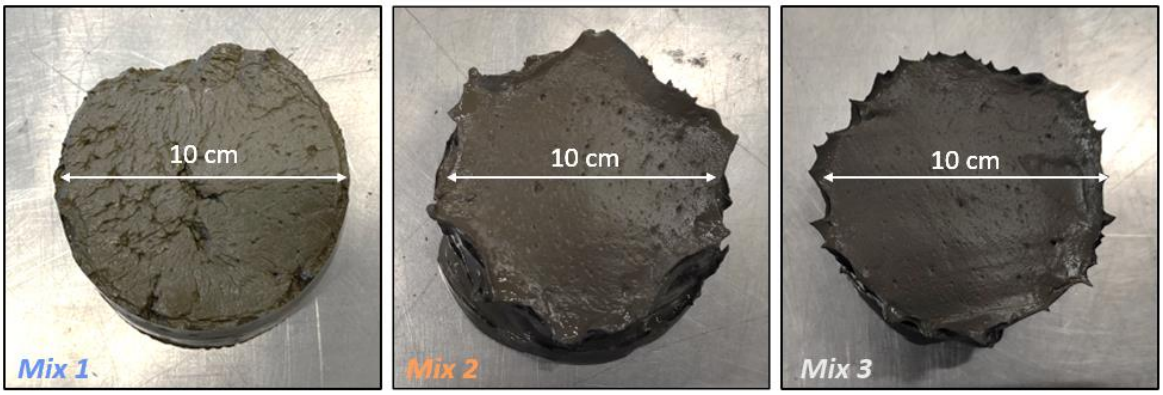

Fig. 4. 1 Slurry mixtures

Table 4. 1. The mixing proportion for the slurry

The volume of the mixture 1 dm³			
Ingredients [gr]	Mix 1	Mix 2	Mix 3
Cement	1606.1	1659.4	1547.7
Water	481.8	462.3	425.8
Superplasticizer	---	3.3	10.8
Silica fume	---	---	154.8
W/C ratio	0.30	0.28	0.28

4.2. Hardened pavers properties

4.2.1. Impact of the cement paste quantity on the thickness of the sample

The objective of this test was to determine the influence of the cement paste amount on the compaction ability of the aggregate/fresh slurry mixture sample and the correlation between flexural strength, void content and slurry quantity.

A constant mass (2.3 kg) of crushed aggregates 3-5 mm (in lab conditions, i.e., the moisture content is 0%) was used for this test, while the amount of cement paste was progressively increased from 17.9 % to 51.2% related to the mass of the aggregate. The compaction process used on the lab-dry aggregates led to the packing of 59.5 % (or equivalently, a void content of 40.5 %). Cement paste from Mix 1, described in section 3.3.1, was used for this test. The mix design, vibration, and compaction procedure remained the same as described in section 3.4. The proportions of the respective mixtures are given in Table 4. 2.

Fig. 4. 2 shows the height of the sample after compaction versus the amount of slurry added (left axis: blue curve) and the void content of the samples (right axis: orange curve). The increase in height after compaction with the amount of slurry added, between 17.9 and 31.3 %, clearly shows that the cement paste is not only located within the voids but also around the aggregates, changing their ability to compact. Also, determining the void content (explained below) in the paste sample shows that the void content decreases from 40.5 (no-paste) to 35 (17.9 % paste), showing that the paste covering the aggregates can deform and be squeezed during compaction. Note that in the 17.9 % paste sample, no flowing of paste to the bottom of the sample has been observed (see appendix 7.1). Another interesting feature in this curve is the non-monotonic evolution of the sample thickness with the cement paste content. Upon increasing the paste content, thickness initially increases. This tends to show that cement paste sticks to the aggregates, increasing their equivalent diameter while getting slightly squeezed (as shown by the evolution of void content), likely improving flexural strength. Between 31 and 38 % of paste content, though, the thickness drops rather abruptly, i.e., the compaction process is suddenly more efficient. Further analysis of the pavers also shows that above 35 % of cement paste, permeability was zero, and further microstructural observation showed accumulation of the paste at the bottom of the sample. These observations tend to show that the sudden drop in thickness of pavers is likely due to cement paste flowing to the bottom of the sample.

Above 31 %, the thickness of the pavers does not increase further with additional paste, demonstrating that at this point, the paste content around the aggregates reached a limit value, and additional paste flows in the voids, filling the voids but not changing the compacted height.

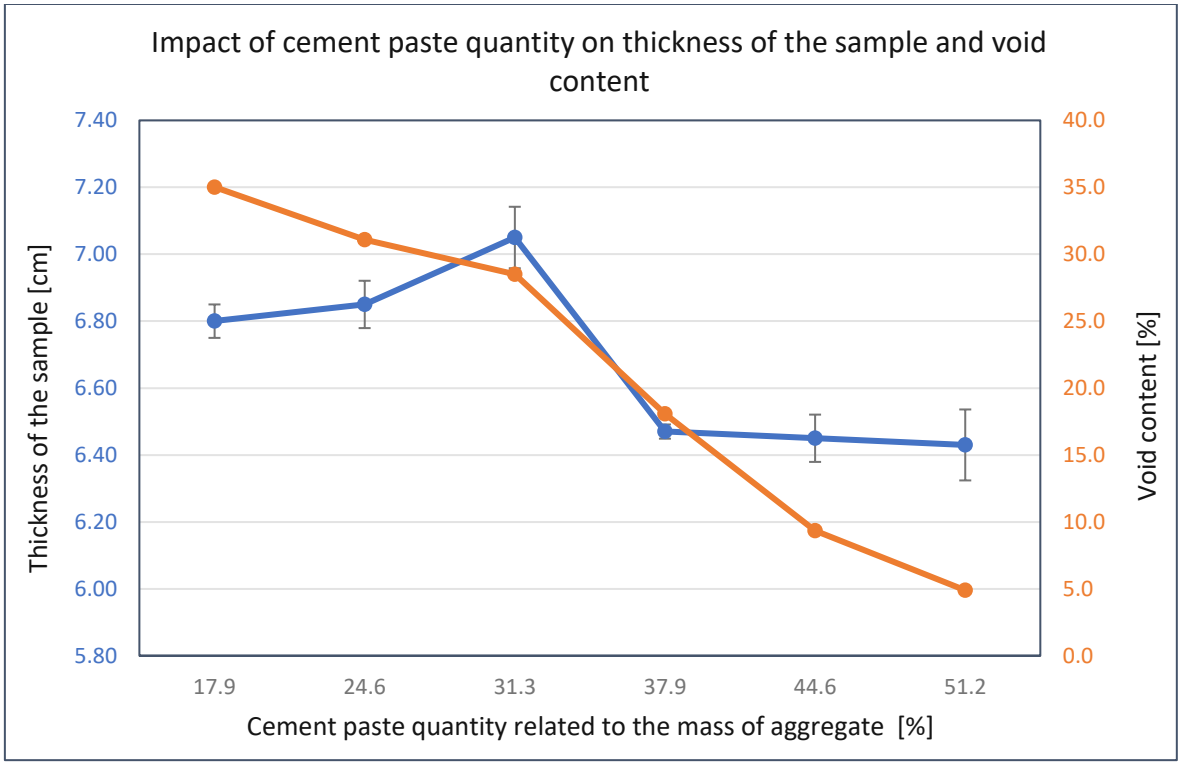

Fig. 4. 2. Impact of cement paste quantity on the thickness of the sample and void content

Fig. 4. 3 shows a schematic illustrating our hypothesis about the compaction process.

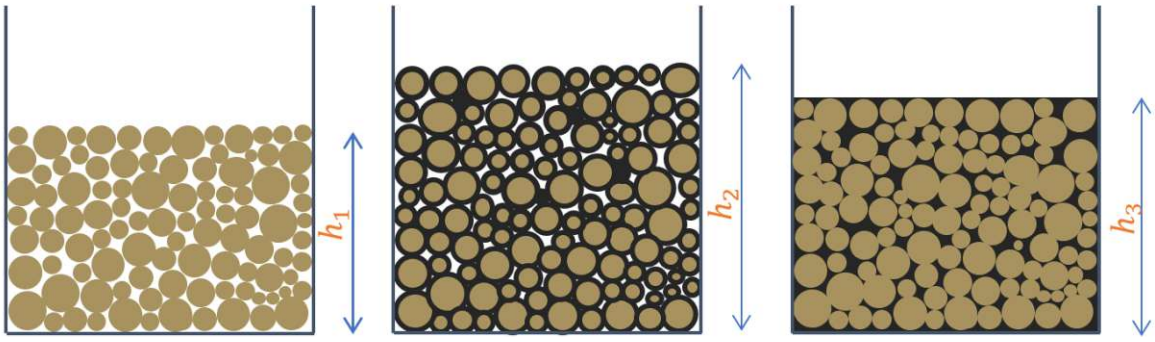

Fig. 4. 3. Influence of the slurry quantity on the compaction of paving stones

Table 4. 2. The proportions of the mixtures for CA 3-5 mm

		Cement paste quantity related to the mass of aggregate [%]					
Ingredients		17.9	24.6	31.3	37.9	44.6	51.2
Cement	kg/m³	232.7	319.8	406.9	492.7	579.7	665.5
Water	kg/m³	69.8	95.9	122.1	147.8	173.9	199.7
CA 3-5	kg/m³	1689.9					

The void content was determined using the liquid displacement method. The dimensions of the sample were measured precisely to determine the bulk volume. Samples were placed in the water to calculate the volume of water needed to fill the voids. The void content was calculated according to the equation *(14)*. The correlation between void content with slurry quantity and flexural strength is shown in Fig. 4. 4

$$\varepsilon = \frac{V_w}{V_b} \qquad (14)$$

ε- void content, in (%)

V_w- volume of water needed to fill the voids, in (m^3)

V_b- bulk volume of the sample, in (m^3)

In this test, it was observed that a minimum void content of 20% is required to achieve adequate water permeability. This value depends on the connectivity of the voids, which is directly related to the quantity of cement paste.

Results show that mechanical properties are as well directly related to the void content. In this test, it was observed that the void content must be below 31 % (24.6 % cement paste of mass of aggregate) to achieve sufficient mechanical properties. The appendix (see 7.1) shows a cross-section of each representative mixture, demonstrating the distribution of voids as a function of slurry quantity.

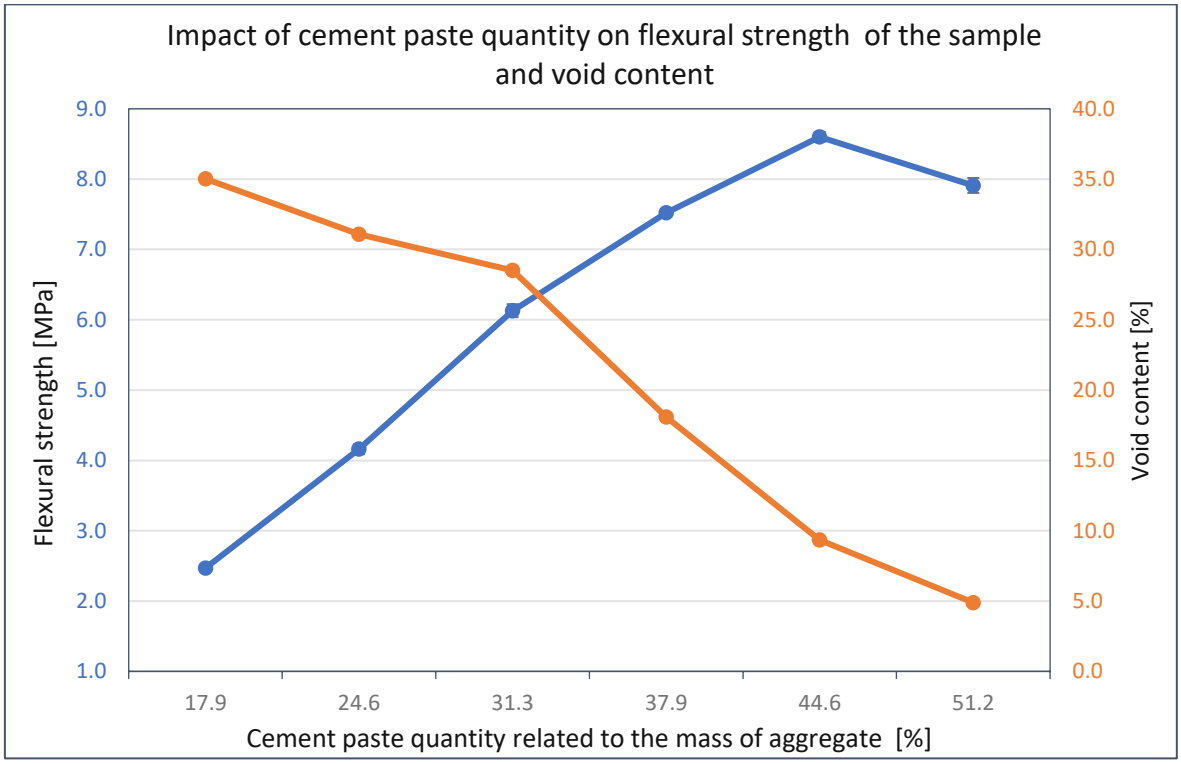

Fig. 4. 4. Impact of cement paste quantity on void content and flexural strength

4.2.2. Influence of slurry quantity on flexural strength

Crushed aggregates of 2-4 mm were used to optimize the amount of slurry. Different amounts of slurry from the mixes explained in section 4.1 were used. The amount of slurry was always related to the mass of aggregate. Mixture proportion with 40% slurry quantity is shown in Table 4. 3, with 35 % slurry quantity in Table 4. 4, and with 30 % slurry quantity in Table 4. 4. Slurry quantity was always related to the mass of the aggregate, and the quantity of aggregate was constant for all mixtures.

Fig. 4. 5 shows the flexural strength for the crushed aggregate 2-4 mm with different slurry content and properties.

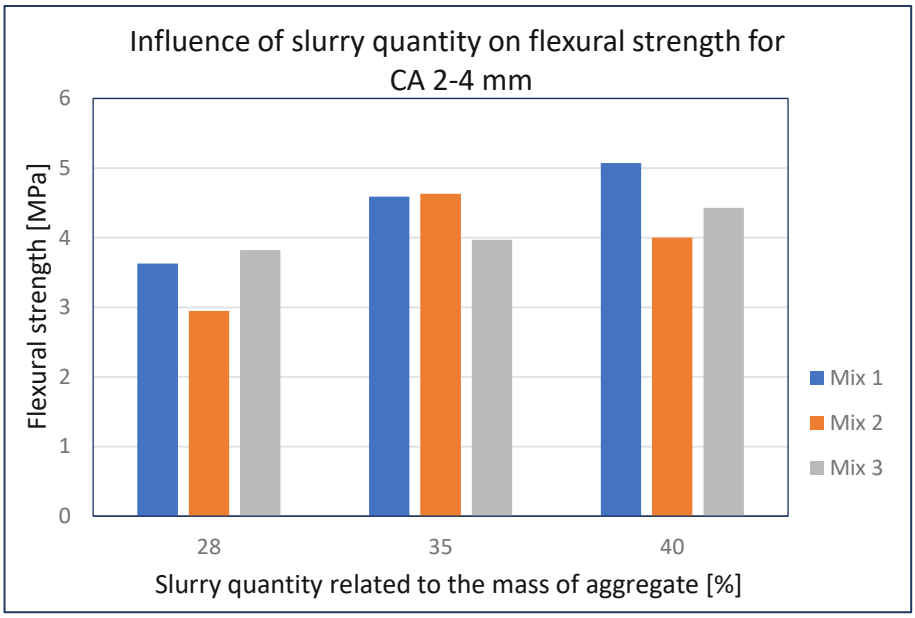

Fig. 4. 5. Optimization of the slurry quantity (Flexural strength for CA 2-4)

In this test, the admixtures were found to have no significant impact on flexural strength. Samples with 40% slurry content related to the mass of the aggregate were nearly impermeable. Due to the vibration and compaction process, the slurry flows into the bottom of the sample blocking the voids as shown in Fig. 4. 7. Samples with a slurry content of 35% have higher water permeability than samples with a slurry content of 40%, but there are still some blocked voids (see Fig. 4. 8) in the bottom of the samples. Fig. 4. 9 shows the uniform distribution of void content for the sample with 28%, which has a water permeability higher than 20 l/m²/s. Fig. 4. 6 shows how the water passes through the permeable paving stone with crushed aggregate 3-5 mm, containing 28 % cement paste, related to the aggregate mass and crushed aggregate content.

In this test, it was observed that the slurry content should be between 28-35%, related to the mass of the aggregate, depending on the size, shape of the aggregate, and compaction process.

Fig. 4. 6. Water permeable paving stone

Table 4. 3.The mixture proportion with 40% slurry quantity

Ingredients		Mix 1	Mix 2	Mix 3
Cement	kg/m³	482.3	489.9	454.4
Water	kg/m³	144.4	136.2	124.4
Superplasticizer	kg/m³	---	1.5	3.2
Silica fume	kg/m³	---	---	45.4
CA 2-4 mm	kg/m³	1567.6		

Table 4. 4. The mixture proportion with 35% slurry quantity

Ingredients		Mix 1	Mix 2	Mix 3
Cement	kg/m³	422.0	428.6	397.6
Water	kg/m³	126.6	119.2	108.7
Superplasticizer	kg/m³	---	0.9	2.8
Silica fume	kg/m³	---	---	39.8
CA 2-4 mm	kg/m³	1567.6		

Table 4. 5.The mixture proportion with 28 % slurry quantity

Ingredients		Mix 1	Mix 2	Mix 3
Cement	kg/m³	337.6	342.9	318.1
Water	kg/m³	101.3	95.4	87.0
Superplasticizer	kg/m³	---	0.7	2.2
Silica fume	kg/m³	---	---	31.8
CA 2-4 mm	kg/m³	1567.6		

Fig. 4. 7. Sample with 40 % slurry quantity related to the aggregate mass.

Fig. 4. 8.Sample with 35 % slurry quantity related to the aggregate mass.

Fig. 4. 9. Sample with 28% slurry quantity related to the aggregate mass.

4.2.3. Influence of the particle size on the flexural strength

In this section, the influence of aggregate size on flexural strength is discussed, and the results are shown in Fig. 4. 10. Different aggregate sizes were used, e.g., river aggregate 1-3 mm and crushed aggregate 2-4, 3-5, and 4-8 mm. **Mix 1,** described in section **3.3.1,** was used for each aggregate type. The quantity of cement paste was the same for each aggregate size, with 30% cement paste related to the aggregate mass. Table 4. 6 shows the mixing proportions for all aggregate types. The mix design, vibration, and compaction procedure remained the same as described in section 3.4. Samples were tested after one days (blue column), after seven days (orange column), and after twenty-eight days (gray column). From the diagram, it can be seen that the flexural strength for all compounds is between 3.4 and 4.6. River aggregate 1-3 has the lowest flexural strength, and the highest flexural strength was achieved with crushed aggregate 3-5 mm.

In this test, it was observed that mixtures with crushed aggregates have a higher flexural strength due to the rougher surface, which provides better adhesion with the cement paste.

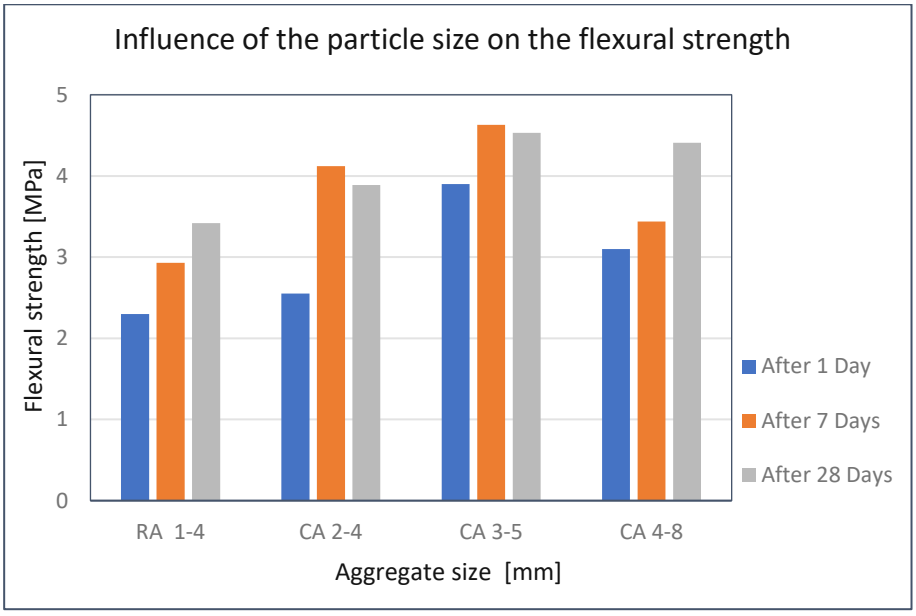

Fig. 4. 10. Flexural strength of samples containing 30 % of cement paste over aggregate mass

The water permeability of these samples was measured as described in Section 3.3, and all the samples have a value higher than 20 l/m²/s (see Table 4. 7).

Table 4. 6.Mixing properties with different aggregate sizes

The volume of the mixture 1 m³				
Ingredients	RA 1-3	CA 2-4	CA 3-5	CA 4-8
Cement kg/m³	373.5	361.7	390.0	390.9
Water kg/m³	112.1	108.5	117.0	117.3
Aggregate kg/m³	1618.6	1567.6	1689.9	1693.8

Table 4. 7. Flexural strength and water permeability

Aggregate size [mm]	Flexural strength [MPa]	Water Permeability [l/m²/s]
RA 1-3	3.4	> 20
CA 2-4	4.1	> 20
CA 3-5	4.6	> 20
CA 4-8	4.4	> 20

5. Conclusions

The work in this thesis is based on optimization and experimental investigation. The objective was to develop a mix design that is suitable to produce water-permeable pavers. During this work, several parameters that influence water permeability and mechanical properties were investigated. The properties of the aggregates used in this study were one of the first parameters explored in this thesis.

It was observed that the packing of aggregate depends on size, shape, amount, and shape and size of the mold (in the appendix (see 7.2) is shown the wall effect on bulk density). The use of a mixture of two different types (e.g., CA 4-8 and RA 1-3) as shown in the appendix (see 7.3) increases the bulk density. The smaller particles fit (i.e., filler grains) between the larger particles and increase the contact points between the aggregates, which results in higher mechanical properties (see Fig. 7.14), but reduces the water permeability (i.e., less inter-particle voids) (see Fig. 7.13).

It was also found that river aggregates can be packed better than crushed aggregates due to their rounder surface, but crushed aggregates provide better mechanical properties than river aggregates due to their rougher surface.

Vibration and compaction energy, as well as the cement paste properties and quantity, are the main parameters that directly affect the distribution of void content, which in turn is linked to the mechanical properties and water permeability of the paving stone. Cement paste flows, blocking the voids (i.e., losing their interconnectivity), creating impermeable layers on the bottom and in the walls of the pavers.

It was found that the cement paste content should be between 28-35 %, based on the mass of the aggregate, depending on the size, shape of the aggregate. It was also found that the void content must be between 20 and 30 % to achieve sufficient water permeability and mechanical properties of the pavers, although it always depends on how the voids are distributed. The admixtures were observed to have no significant effect on improving the mechanical properties of the pavers.

The mechanical properties, water permeability, and void content of the pavers are interrelated and directly dependent on the quantity and properties of the cement paste, vibration, and compaction energy. The relationship between all these parameters still needs to be studied and optimized.

6. References

[1] M. Sonebi, M. Bassuoni, and A. Yahia, "Pervious concrete: Mix design, properties and applications," *RILEM Tech. Lett.*, vol. 1, pp. 109–115, 2016, doi: 10.21809/rilemtechlett.2016.24.

[2] A. K. Chandrappa and K. P. Biligiri, "Comprehensive investigation of permeability characteristics of pervious concrete: A hydrodynamic approach," *Constr. Build. Mater.*, vol. 123, pp. 627–637, 2016, doi: 10.1016/j.conbuildmat.2016.07.035.

[3] Y. Qin, Y. He, J. E. Hiller, and G. Mei, "A new water-retaining paver block for reducing runoff and cooling pavement," *J. Clean. Prod.*, vol. 199, pp. 948–956, 2018, doi: 10.1016/j.jclepro.2018.07.250.

[4] D. Daneshvar, K. Deix, and A. Robisson, "Effect of casting and curing temperature on the interfacial bond strength of epoxy bonded concretes," *Constr. Build. Mater.*, vol. 307, p. 124328, 2021, doi: 10.1016/j.conbuildmat.2021.124328.

[5] P. Chindaprasirt, S. Hatanaka, T. Chareerat, N. Mishima, and Y. Yuasa, "Cement paste characteristics and porous concrete properties," *Constr. Build. Mater.*, vol. 22, no. 5, pp. 894–901, 2008, doi: 10.1016/j.conbuildmat.2006.12.007.

[6] J. T. Kevern, V. R. Schaefer, K. Wang, and M. T. Suleiman, "Pervious concrete mixture proportions for improved freeze-thaw durability," *J. ASTM Int.*, vol. 5, no. 2, pp. 1–12, 2008, doi: 10.1520/JAI101320.

[7] "Friedl Steinwerke GMBH", [Online]. Available: https://www.steinwerke.at/

[8] "Pavement (architecture)", [Online]. Available: https://en.wikipedia.org/wiki/Pavement_(architecture)

[9] M. K. Bakri and V. Vart, "A critical review on fire resistance structures," pp. 90–92.

[10] "Paver Blocks - Types, Shapes, Uses, and Benefits", [Online]. Available: https://theconstructor.org/building/paver-blocks-types-shapes-uses-and-benefits/39188/

[11] "Globi M.I,", [Online]. Available: http://www.globi-mi.com/

[12] "How Does Permeable Pavement Work?", [Online]. Available: https://www.youtube.com/watch?v=ERPbNWI_uLw

[13] "RVS081801 Pflasterstein- und Pflasterdecken.pdf."

[14] Friedl Steinwerke GMBH, "Terrassenplatten verlegen auf Drainagebeton", [Online]. Available: https://www.youtube.com/channel/UChKjXY66OBtrF-GPqBqXqYQ

[15] "RVS030863 Oberbaubemessung.pdf."

[16] Concrete paving blocks - Requirements and test methods, “ÖNORM EN 1338,” 2007.

[17] “Manufacturing process of paving stones.” [Online]. Available: https://www.youtube.com/watch?v=fMyI4IKRNUg

[18] “Datasheet: Karawanken Zement CEM I 42,5 R C3A free. 2020;,” pp. 2–3, [Online]. Available: https://zement.wup.at/wp-content/uploads/2020/09/PDB_Karawanken-Zement_DE_07_2020.pdf

[19] D. K. Panesar, *Supplementary cementing materials*. Elsevier LTD, 2019. doi: 10.1016/B978-0-08-102616-8.00003-4.

[20] “Product Data Sheet Uses,” *Elkem-Microsilica-940-U,* vol. 3, no. 01, pp. 6–7, 2011.

[21] G. A. Rao, “Investigations on the performance of silica fume-incorporated cement pastes and mortars,” *Cem. Concr. Res.*, vol. 33, no. 11, pp. 1765–1770, 2003, doi: 10.1016/S0008-8846(03)00171-6.

[22] T.Liberto, “Werkstoffe im Bauwesen Laborübung : ‘Frisch- und Festbeton’,” 2020.

[23] A. Institute, A.S., ÖNORM EN 1097-6 , Tests for mechanical and physical properties of aggregates; Part 6: Determination of particle density and water absorption. 2020: Vienna, “ÖNORM EN 1097-6,” 2020.

[24] E. Wolfgang, *"Einfluss der Verdichtung von Kalk-Sand-Rohmassen auf die Scherbenrohdichte von Kalksandstein*.

[25] “ÖNORM EN 1097-3 Tests for mechanical and physical properties of aggregates - Part 3: Determination of loose bul k density and voids,” 2004.

[26] “Mortar Mixer ToniMIX Visco Expert – Model 6226”, [Online]. Available: https://tonitechnik.com/product/mortar-mixer-tonimix-visco-expert-model-6226/

[27] Normungsinstitut, W. Copyright, and A. Standards, “ÖNORM EN 196-1,” 2016.

[28] “Eirich Laboratory Mixer.pdf.” [Online]. Available: https://www.eirich.com/en/processes/mixing-technology/laboratory-mixer/type-el5-eco/

[29] “Prüfung der Biegezugfestigkeit”, [Online]. Available: https://www.betontechnische-daten.de/de/11-2-3-pruefung-der-biegezugfestigkeit

[30] “Permeability Test”, [Online]. Available: https://uta.pressbooks.pub/soilmechanics/chapter/permeability-test/

7. Appendix

7.1. Influence of slurry quantity on void distribution

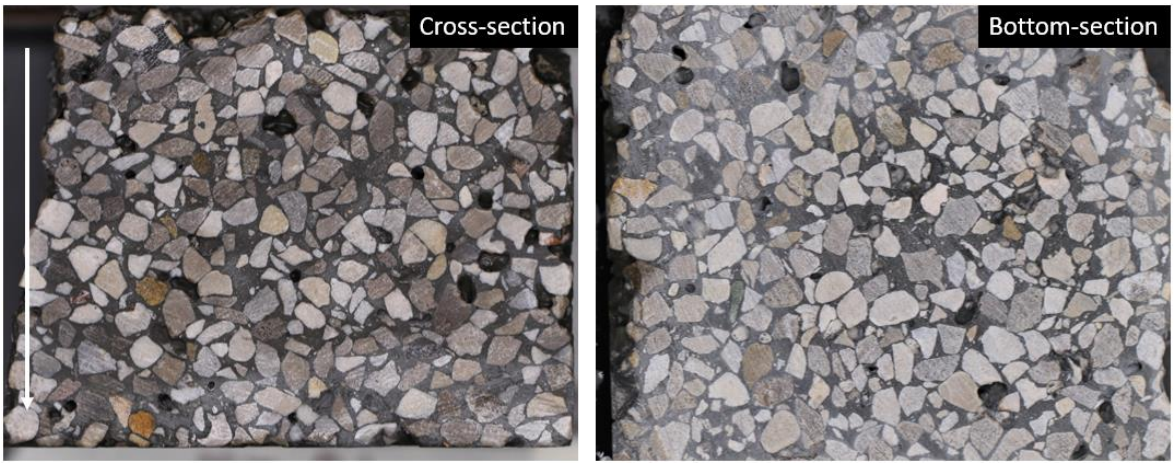

Fig. 7. 1.Sample with a content of 51.2 % slurry, based on the total mass of aggregate

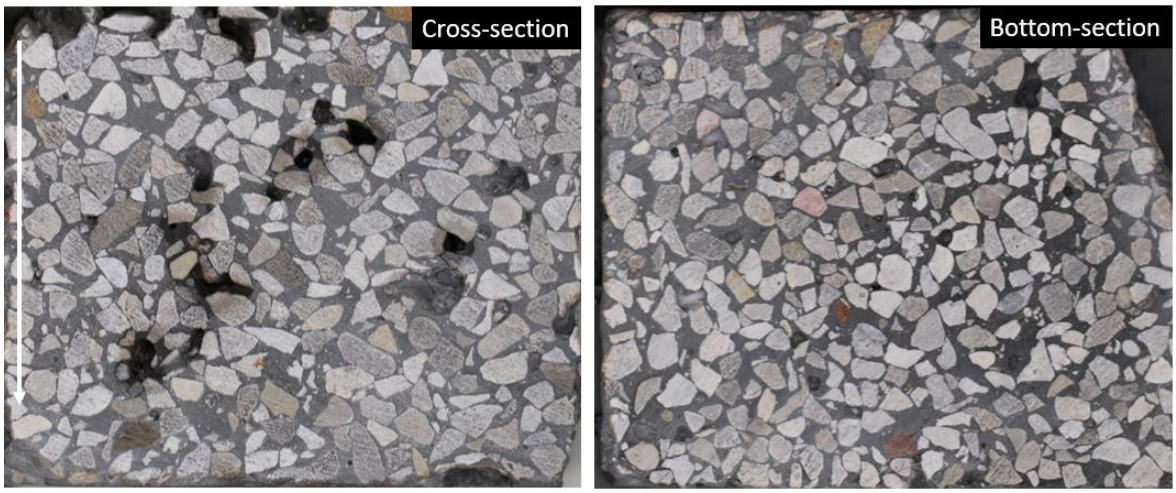

Fig. 7.2. Sample with a content of 44.6% slurry, based on the total mass of aggregate

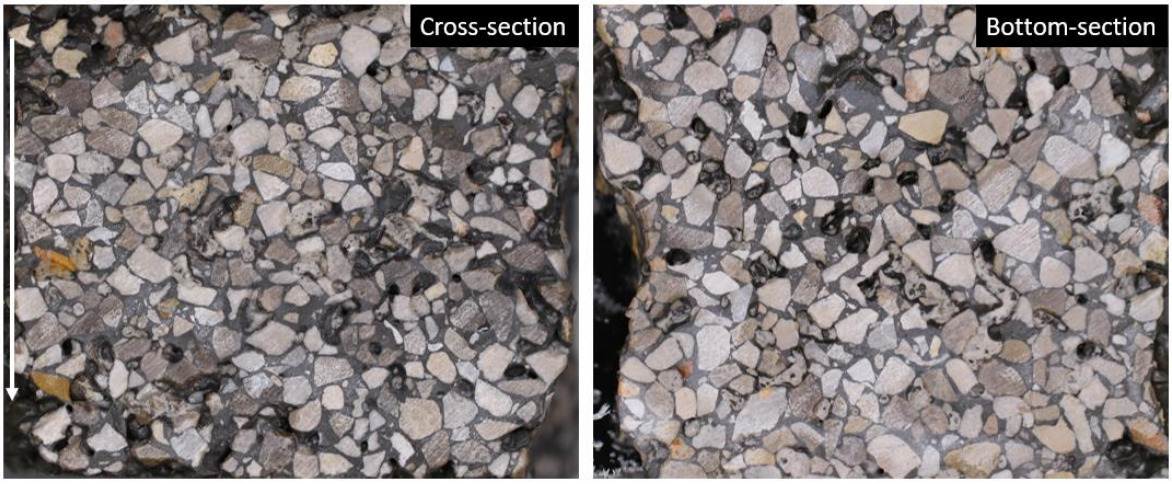

Fig. 7.3. Sample with a content of 37.9% slurry, based on the total mass of aggregate

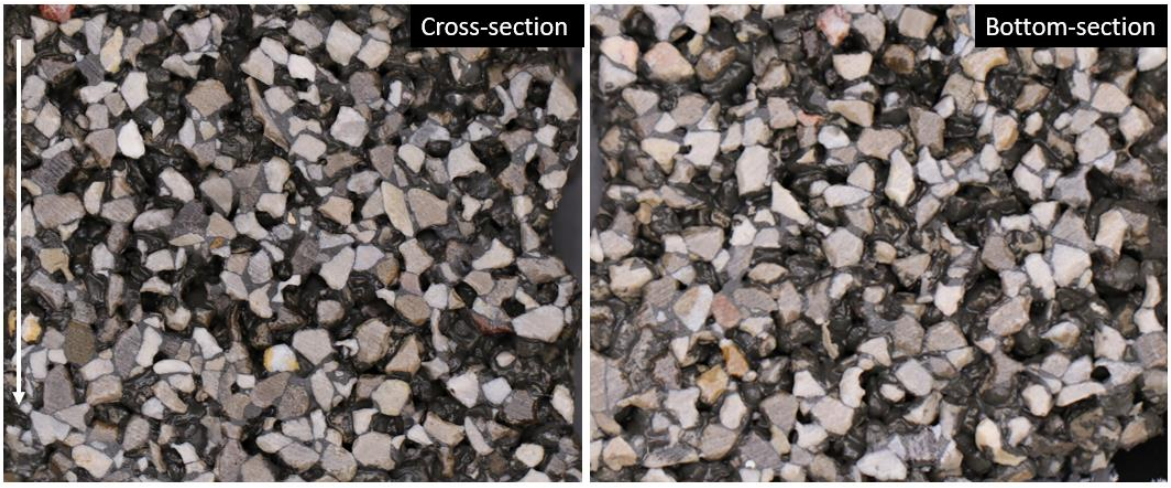

Fig. 7. 4. Sample with a content of 31.3% slurry, based on the total mass of aggregate

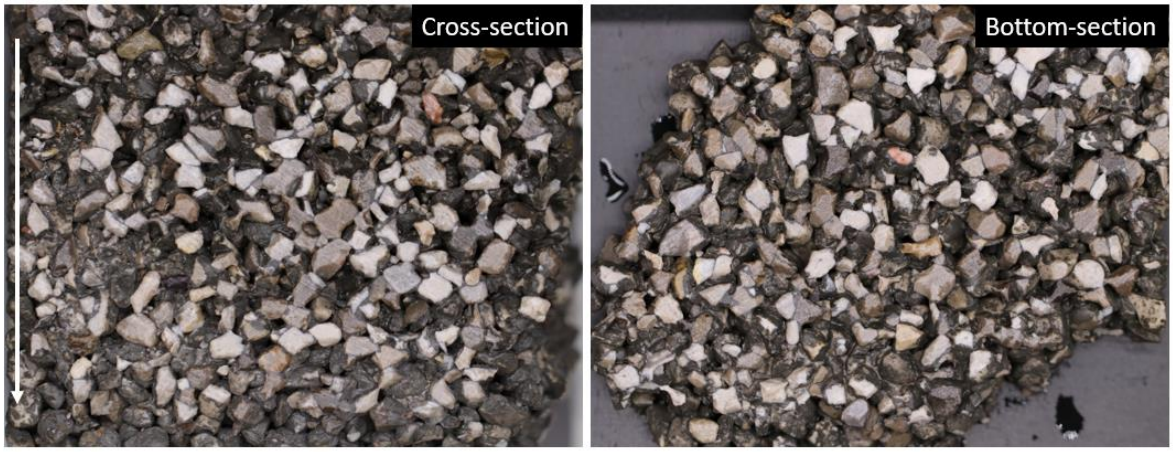

Fig. 7.5. Sample with a content of 24.6% slurry, based on the total mass of aggregate

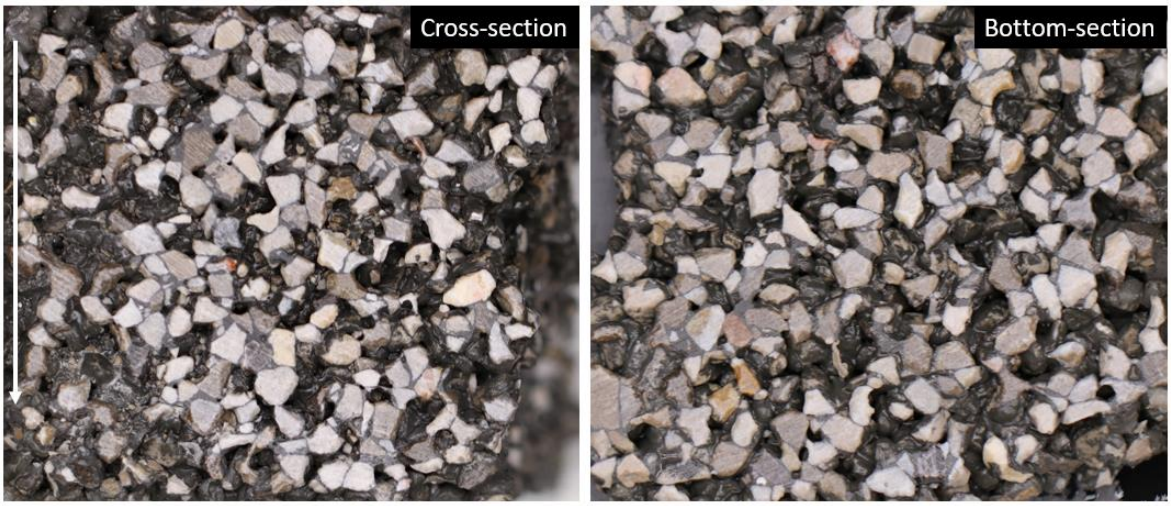

Fig. 7.6. Sample with the content of 17,9 % slurry, based on the total mass of aggregate

7.2. Influence of the wall effect

The procedure is the same as described in the section **3.2.3**

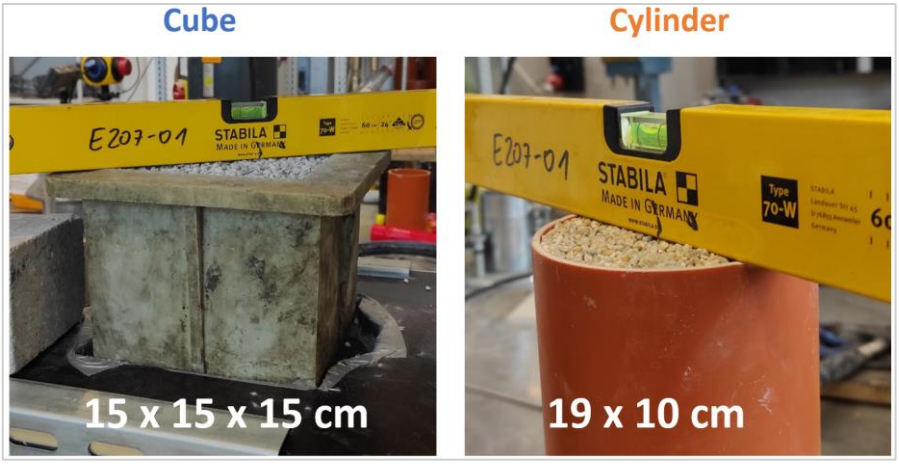

Fig. 7. 7. Cube and cylindrical molds

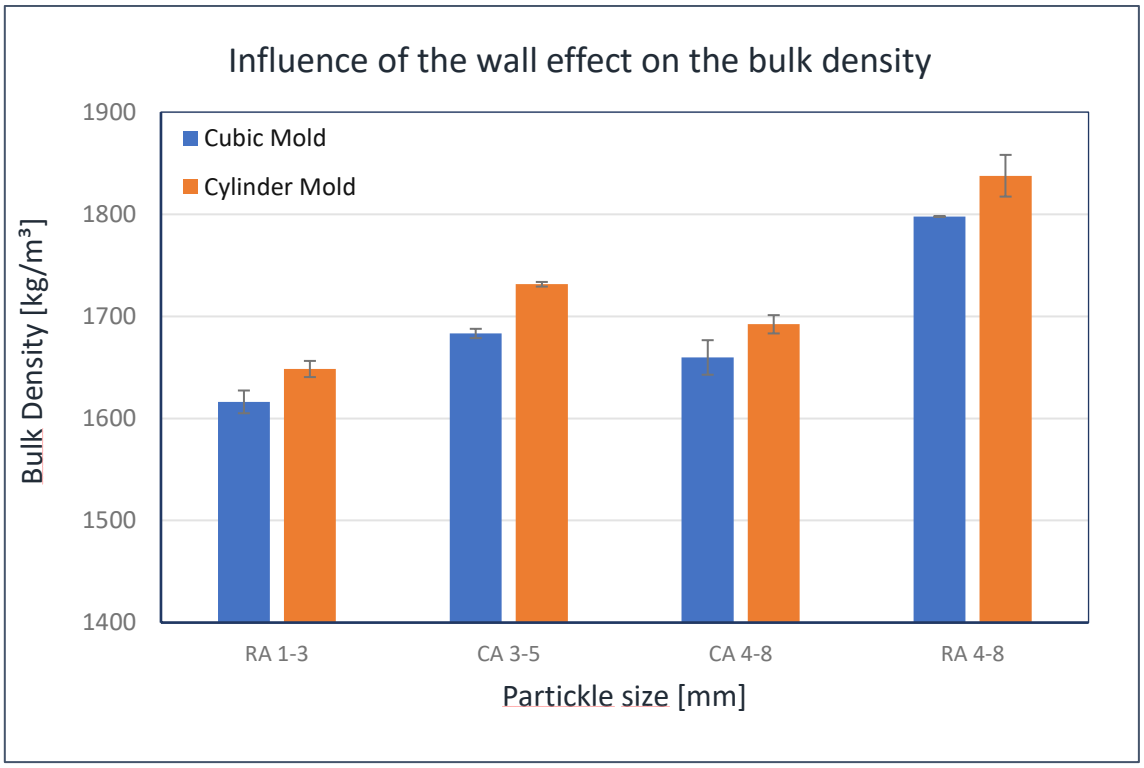

Fig. 7.8. Influence of the wall effect on the bulk density

The surface of the cylinder $A_W = 2\pi r * (h + r) = 781,\ 05 cm^2$

Cube surface $A_W = 6 * (a * b) = 1350,00\ cm^2$

7.3. The mixture of two types of aggregates

Two different aggregates were mixed in an Eirich mixer for 90 s. (RA 1-3 with CA 4-8 and RA 1-3 with RA 4-8). After that, the procedure was the same as described in section **3.2.3.** The results are shown below.

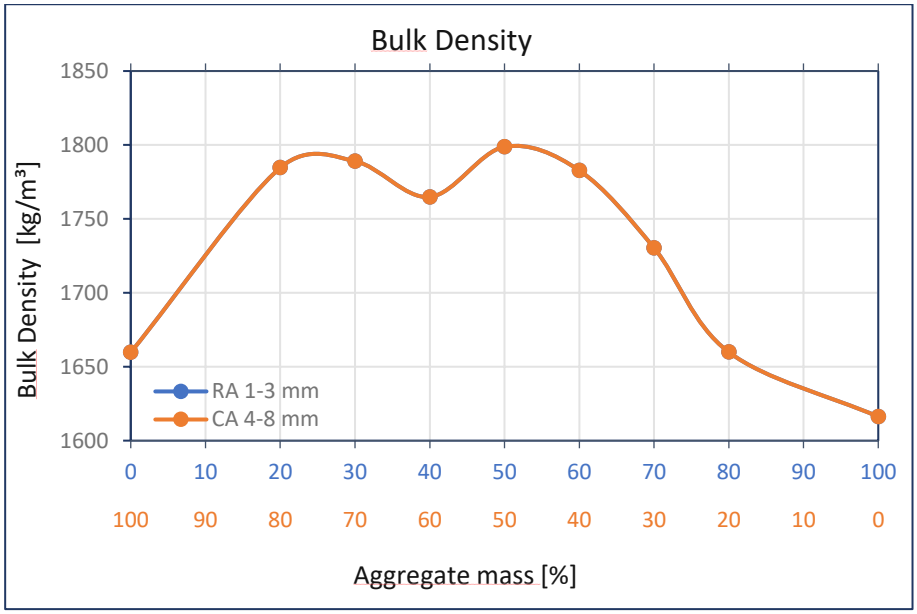

Fig. 7.9. The mixture of two aggregates: Bulk density for the mixture RA 1-3 with CA 4-8

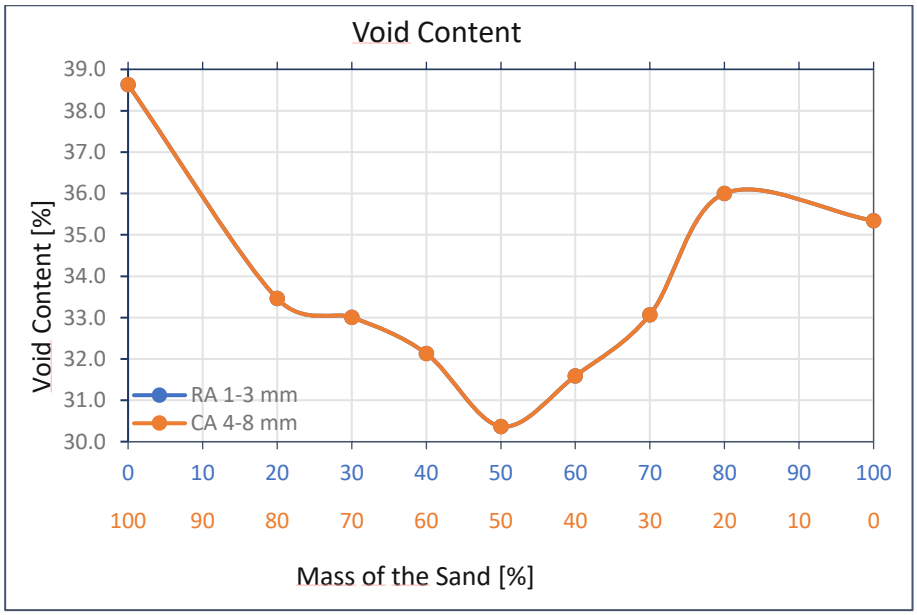

Fig. 7.10. The mixture of two aggregates: Void content for the mixture RA 1-3 with CA 4-8

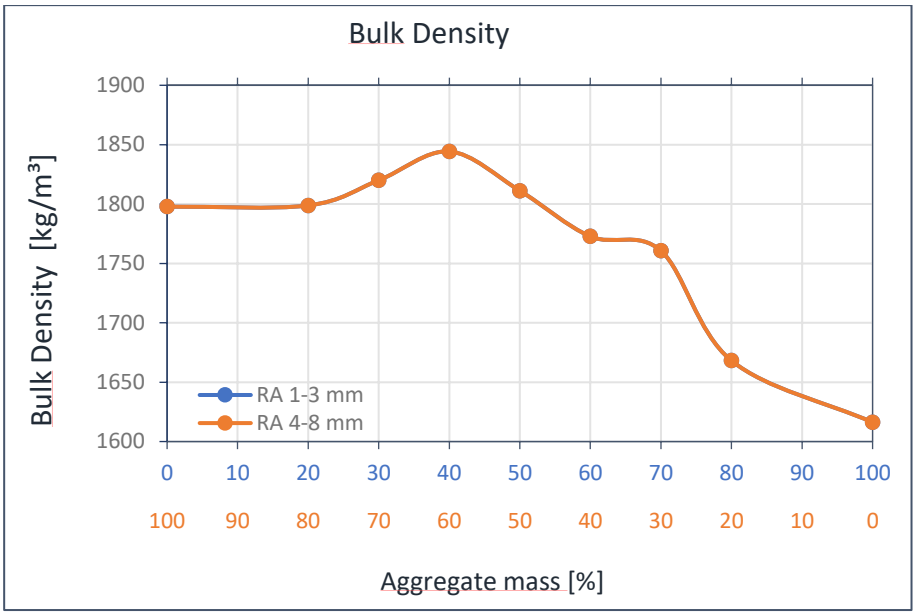

Fig. 7.11. The mixture of two aggregates: Bulk density for the mixture RA 1-3 with RA 4-8

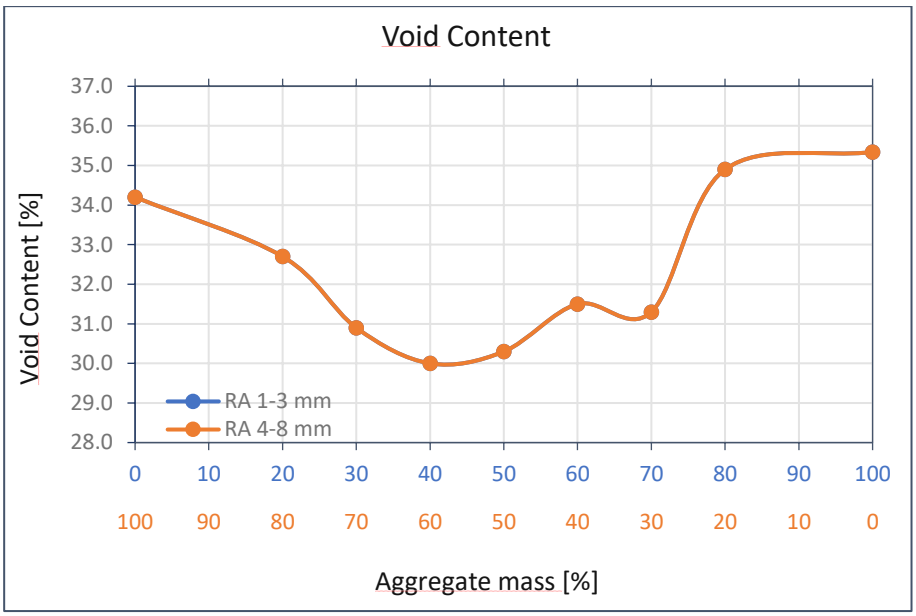

Fig. 7.12. The mixture of two aggregates: Void content for the mixture RA 1-3 with CA 4-8

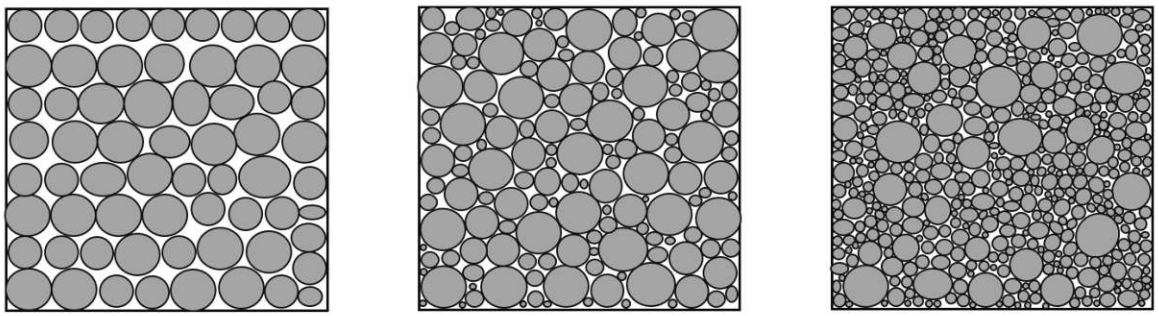

Fig. 7.13. Impact of filler grain in interparticle voids

7.4. Mixture with two different aggregates

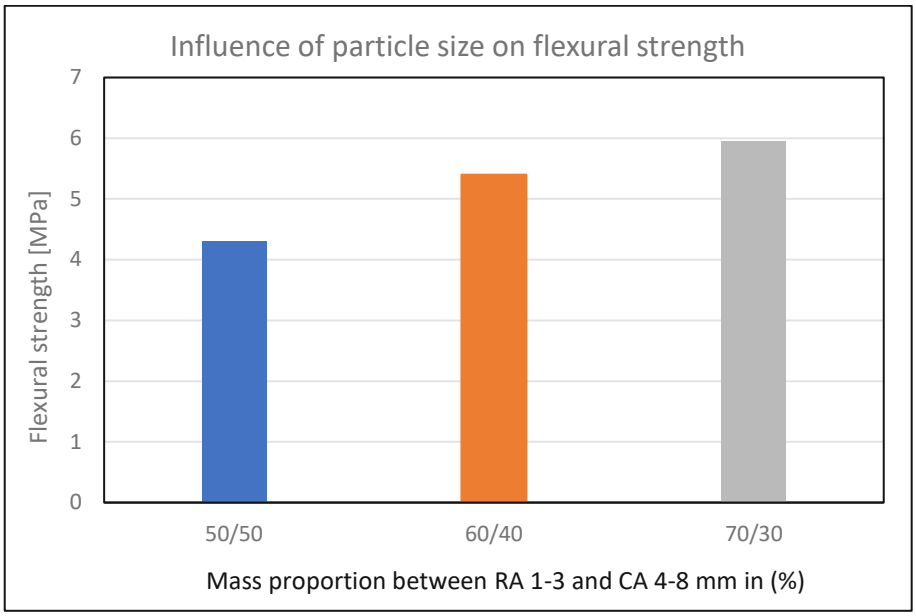

Fig. 7.14. Mixture with two different aggregates: Flexural strength

Table 7. 1. The material proportion for the mixtures with two types of aggregates

Ingredients		Mix 1	Mix 2	Mix 3
Cement	kg/m³	274.6	274.6	274.6
Water	kg/m³	66.6	66.6	66.6
Superplasticizer	kg/m³	6.9	6.9	6.9
Silica fume	kg/m³	27.5	27.5	27.5
Lime Stone 3	kg/m³	82.4	82.4	82.4
RA 1-3	kg/m³	922.2	1106.6	1291.4
CA 2-4	kg/m³	957.0	765.3	574.8
W/C ratio		0.26		

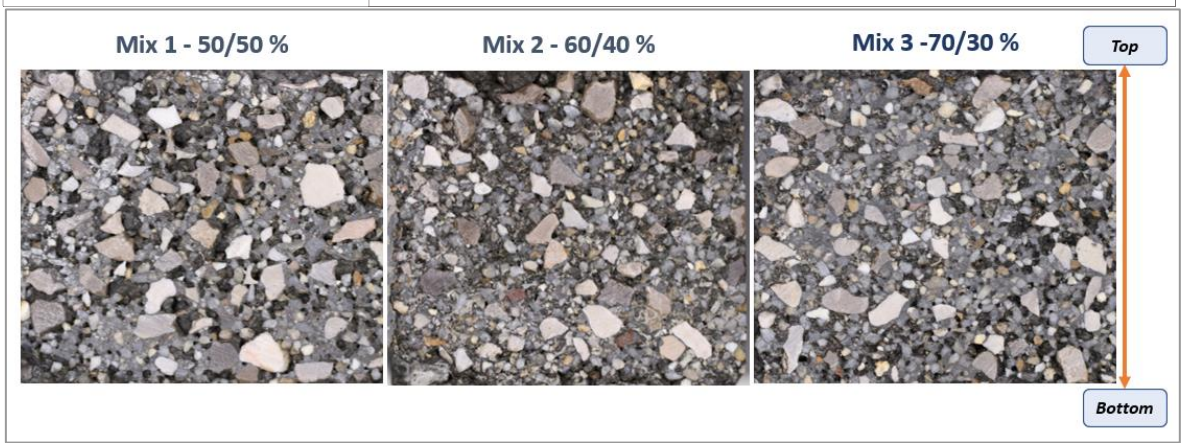

7.5. Particle size distribution (image analysis)

A certain number of particles (approx. 100) from RA 1-3, RA 4-8, RA 8-16, CA 3-5, and CA 4-8 were taken for image analysis using Image J, which measures the area, perimeter, maxFeret, minFeret. By which the diameter was calculated, assuming that all particles have a spherical shape in order to calculate the volume of particles. The volume of the same particles was measured with a pycnometer to determine the difference. The following figures are shown the difference obtained from Image J and Pycnometer. The blue column is the volume obtained from the pycnometer, the blue plus orange column is the volume calculated from Image J, and the orange column is the difference.

It was found that the volume of the particles measured with the pycnometer and the volume calculated with Image J for the same particles were in the range of 20-70% for all types of aggregates investigated.

Determination of the particle size distribution with Image J was not possible because of the large difference between the real volume measured with the pycnometer and the volume calculated with Image J.

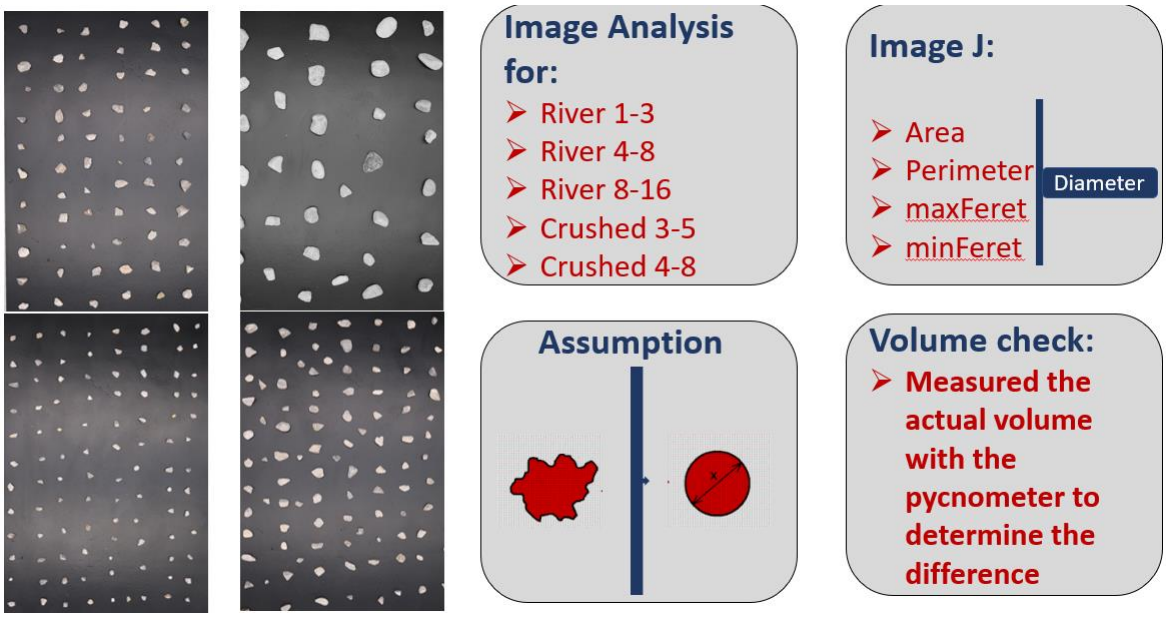

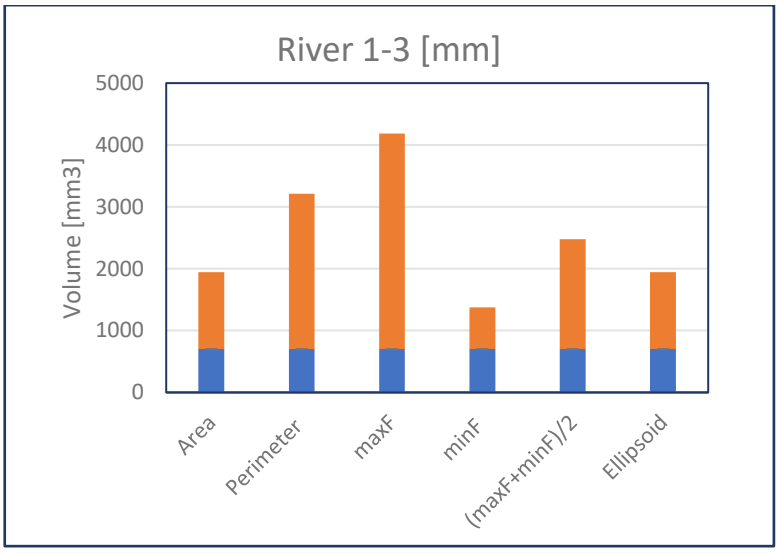

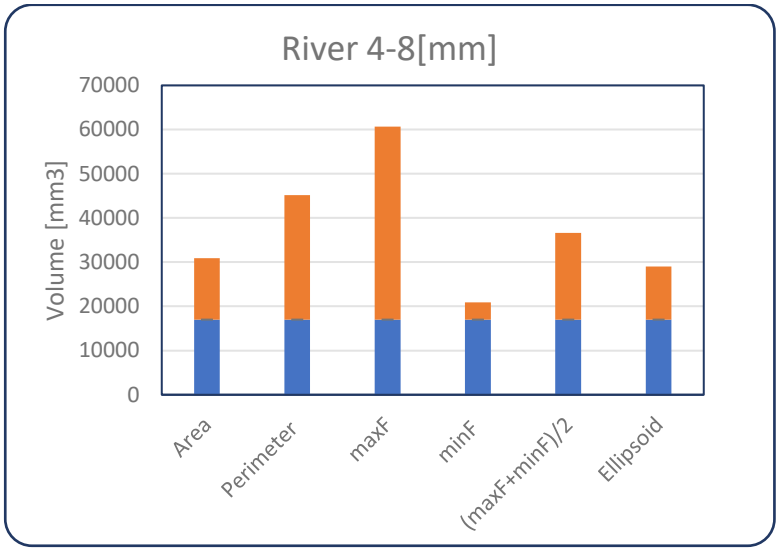

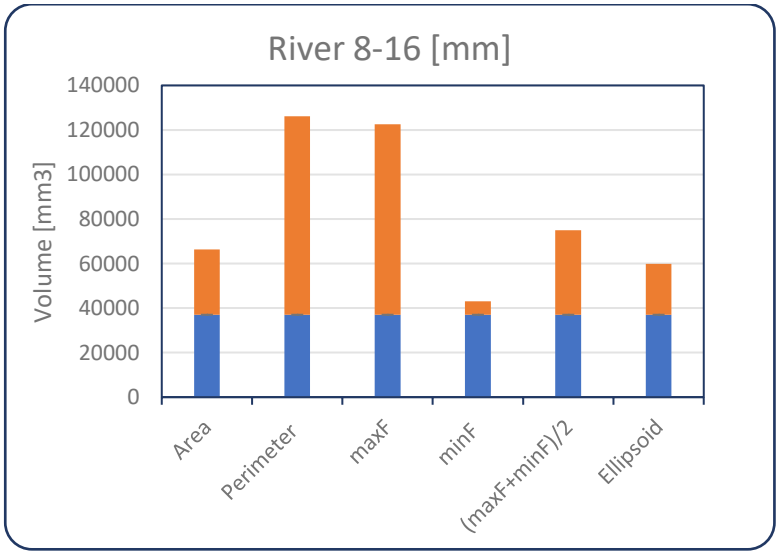

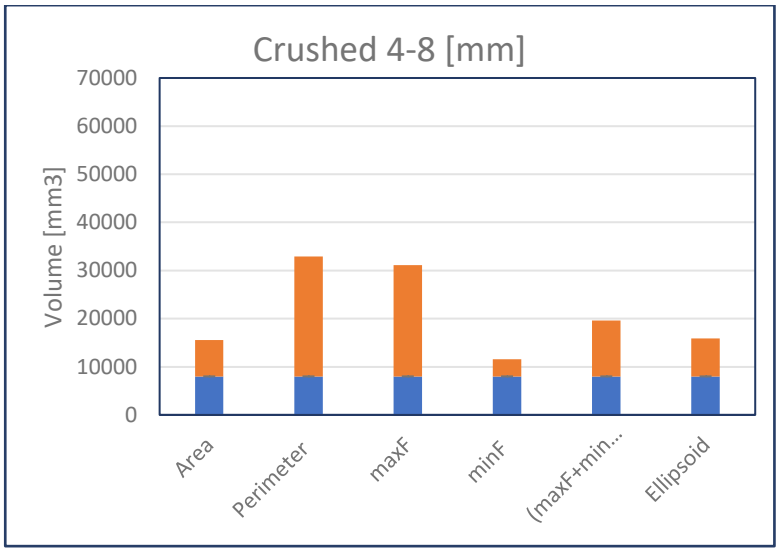

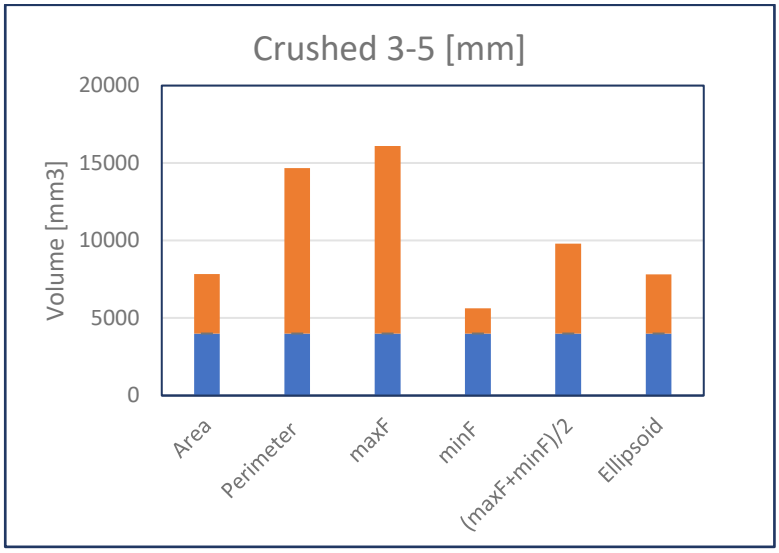

7.6. The derived equation for the saturated surface dry particle density

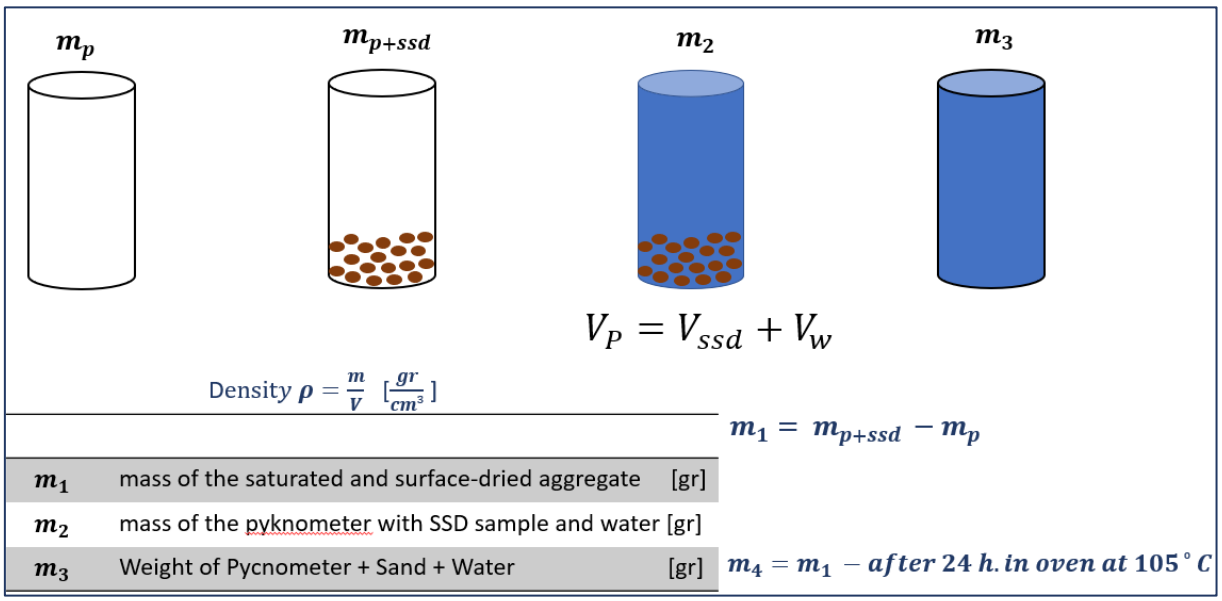

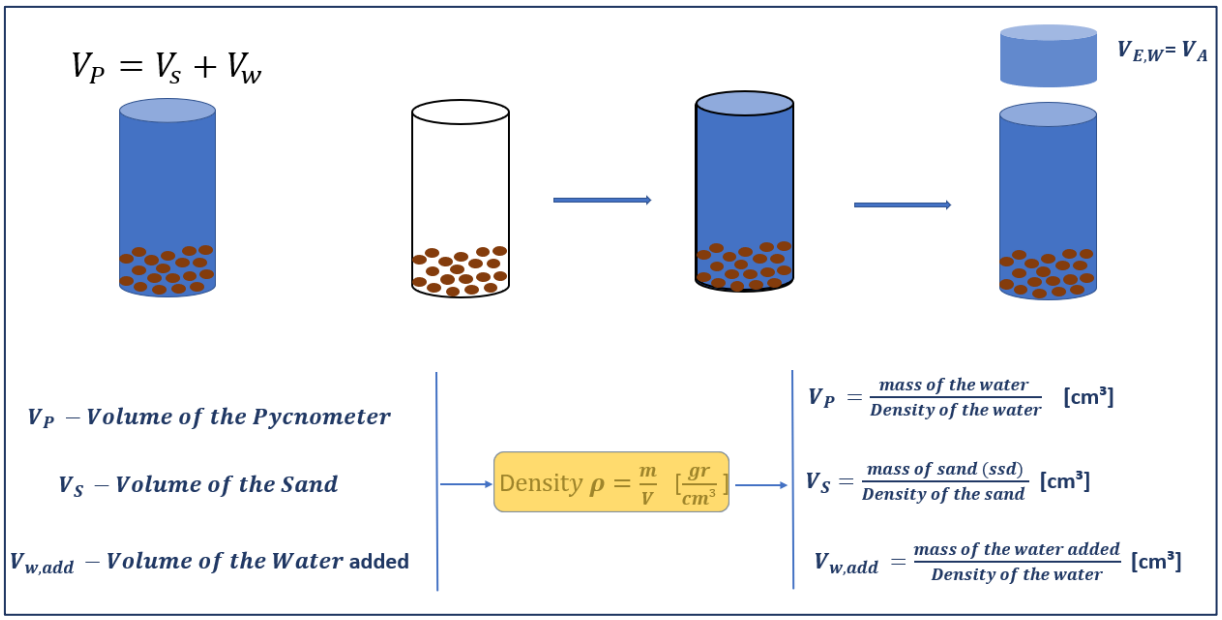

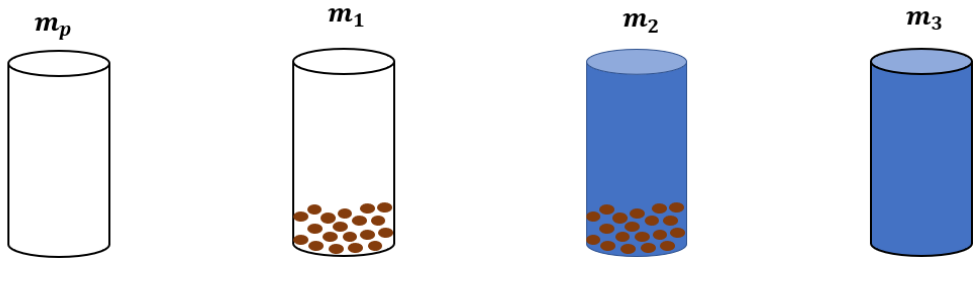

$$V_P = V_S + V_w$$

$$\frac{\text{mass of the water}}{\text{Density of the water}} = \frac{\text{mass of the sand}}{\text{Density of the sand}} + \frac{\text{mass of the water addet}}{\text{Density of the water}}$$

$\rho_{ssd} = ?$

Density of the water $\rho_{ssd} \approx 1 \frac{gr}{cc}$ (22 ± 3) °C – ÖNORM_1097-6:2020 (E) (page 49)

Mass of the water: $m_3 - m_p$

Mass of the sand : $m_1 - m_p$

Mass of the added water: $m_2 - m_1$

$$\frac{\text{mass of the water}}{\text{Density of the water}} = \frac{\text{mass of the sand}}{\text{Density of the sand}} + \frac{\text{mass of the water addet}}{\text{Density of the water}}$$

$$\frac{m_3 - m_p}{\rho_w} = \frac{m_1 - m_p}{\rho_{ssd}} + \frac{m_2 - m_1}{\rho_w}$$ → ρ_w= 1 gr/cc at Temp 23 ± 2, $m_p = 0$ (*mass of the Pycnometer*)

$$m_3 = \frac{m_1}{\rho_{ssd}} + m_2 - m_1$$

$$m_3 - m_2 + m_1 = \frac{m_1}{\rho_{ssd}}$$

$$\rho_{ssd} = \frac{m_1}{m_3 - m_2 + m_1}$$

$$\rho_{ssd} = \frac{m_1}{m_1 - (m_2 - m_3)}$$

7.7. Excel-sheet model for mixture calculation

Mischungsberechnung für wasserdurchlässige Pflastersteine

durchgeführt von :	Meriton Ramizi	Datum:	Dez 21	Ort :	Wien
Zweck:	Diplomarbeit-Friedl Steinwerke				

◊ Gold hinterlegte Felder müssen eingetragen werden ◊

Eingabewerte			Eigenschaften von Sand		
Sand ==>	Kant Korn 3-5		Hohlraumgealt	[%]	40.5
W/Z-wert ==>	0.30		Schüttdichte	[kg/m³]	1689.9
Hohlräume.G.mit Matrix[%] ==>	100.0	35.77	Rohdichte	[kg/m³]	2842.0
Dicke der Stein [cm] ==>	6.0		Wasser gehalt	[M . %]	0.0
Länge der Stein [cm] ==>	15.0		Wasser gehalt	[l/m³]	0.0
Breite der Stein [cm] ==>	15.0		Feucht Masse	[kg/m³]	1689.9

Kennwerte.

Volumen Sand	[dr	0.80	Matrix bezogen auf die Masse	[M. %	50.04
Volumen Holräume	[dr	0.55	Matrix bezogen auf das Volumen	[V. %	68.07
Masse des Sandes	[g	2281.37	Volumen der Probekörper	[dm³	1.35

Stoffraum

	Anteil [V. %]	Anteil [M. %]	Masse [kg]	Rohdichte [kg/dm³]	Stoffraum [dm³]
Hohlraumgehalt	0.0	0	0	0.00	0.0
Matrix	40.5	33.35	845.7	2.09	405.0
Zuschläge	59.5	66.65	1689.9	2.84	595.0
Frischbetonrohdichte [kg/m³]	**100.0**	100.0	2535.6	4.9	1000.0
Wasserzugabe gesamt [l/m³]					

Zutaten	Bezeichung	Anteile [M.1]	Anteile [V.1]	Masse [kg]	Rohdichte [kg/dm³]	Stoffraum [dm³]
Fließmittel	ACE 430	0	0.0	0.0	1.06	0.0
Zement	Cem I 52,5 N C3A-frei	100	32.3	650.5	3.10	209.8
Kalkstein	KSM H100	0	0.0	0.0	2.71	0.0
Silikastaub Pulver	Elkem 940 U	0	0.0	0.0	2.30	0.0
Silikastaub Flüssig	REBA	0	0.0	0.0	1.35	0.0
Wasser inkl. Fließmittel	Flüssigkeiten	30	30.0	195.2	1.00	195.2
		130	62.3	845.7	2.09	405.0

Zuschläge

Sand [mm]	Hohlraumgealt [%]	Schüttdichte [kg/m³]	Rohdichte [kg/m³]	Wasser Gehalt [M . %]	[l/m³]	Feucht-M. [kg/m³]
Rund Korn 1-2	39.6	1601.3	2660.7	0	0.0	1618.6
Rund Korn 1-3	40.0	1618.6	2657.0	0	0.0	1618.6
Kant Korn 2-4	43.2	1567.6	2779.0	0	0.0	1567.6
Kant Korn 3-5	40.5	1689.9	2842.0	0	0.0	1689.9
Kant Korn 4-8	41.2	1693.8	2880.9	0	0.0	1693.8

Mischung

Volumen der Mischung für einen Stein [dm³] ==>		1.35	1.0	<== Volumen der Mischung [m³]
	Bezeichung	[gr]	[kg]	**Mischreihenfolge und Dauer**
Wasser	Leitungswasser	263.5	195.2	Mischertyp: Eirich R 02 Vac
				Wirblertyp: Stiftenwirbler
Fließmittel	ACE 430	0.0	0.0	
				Mischreihenfolge:
Zement	Cem I 52,5 N C3A-frei	878.2	650.5	
				Zeit [s] / Drehungen [U/min]
Silikastaub Pulver	Elkem 940 U	0.0	0.0	
Silikastaub Flüssig	REBA	0.0	0.0	
				CEM+MS+S: 90 / 200
Kalkstein	KSM H100	0.0	0.0	
				W+FM: 30 / 200
Sand	Kant Korn 3-5	2281.4	1689.9	
				Mischen: 90 / 200
	Masse	**3423.0**	2535.6	Summe: 210